UNIVERSITY OF CAMBRIDGE

Scanning Precession Electron Diffraction

Duncan N. Johnstone
Department of Materials Science & Metallurgy

Electron Microscopy Group
www-hrem.msm.cam.ac.uk

Acknowledgement: Paul A. Midgley (for slides and wisdom)

Outline

1. Practical problems and precession
2. Precession Electron Diffraction
3. Experimental aspects of PED
4. Scanning Precession Electron Diffraction
5. Scanning Precession Electron Tomography

UNIVERSITY OF CAMBRIDGE

Part I: Practical Problems & Precession

Traditional Applications of Electron Diffraction

Structure Solution and Refinement

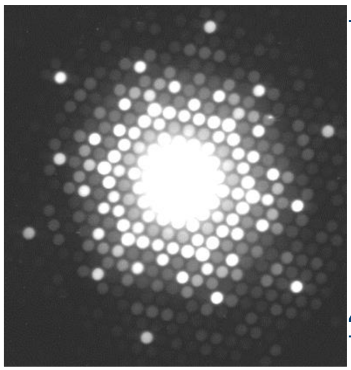

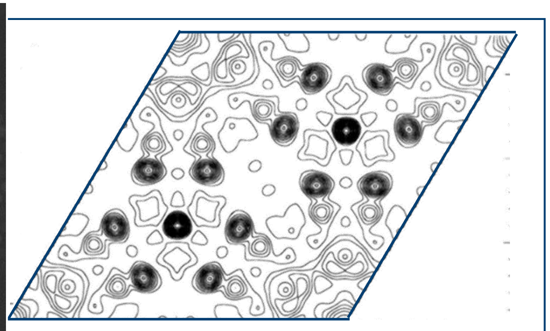

Beryl - $Be_3Al_2Si_6O_{18}$

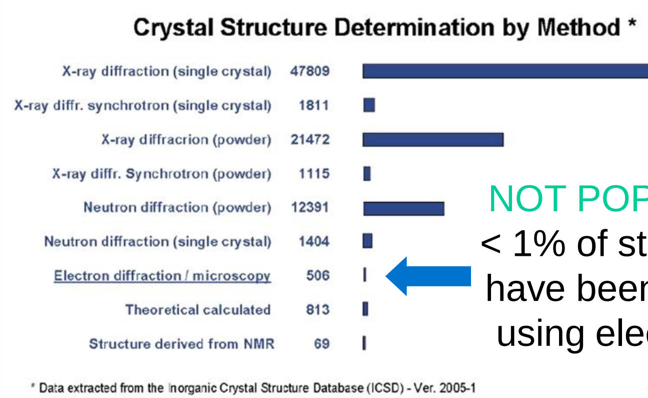

NOT POPULAR!!
< 1% of structures have been solved using electrons !

Point Group and Bravais Lattice Identification

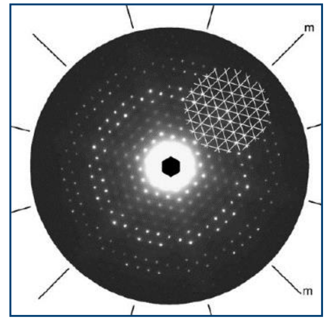

J.P. Morniroli et al. *Ultramicroscopy* 107 (2007) 514–522

Laue class	$\bar{1}$	2/m	mmm	4/m	4/mmm	$\bar{3}$	$\bar{3}$m	6/m	6/mmm	m$\bar{3}$	m$\bar{3}$m
					and absence of 3m (6mm)		and absence of 4mm (4mm)			and presence of 2mm (2mm)	and presence of 4mm (4mm)
Highest "ideal" symmetry	1 (2)	2 (2)	2mm (2mm)	4 (4)	4mm (4mm)	3 (6)	3m (6mm)	6 (6)	6mm (6mm)	3 (6)	3m (6mm)

Table 1. Connection between the "ideal" symmetry of microdiffraction precession patterns and the Laue class. ZOLZ symmetries are given between parentheses.

Crystal Cartography

Phase & Orientation Mapping

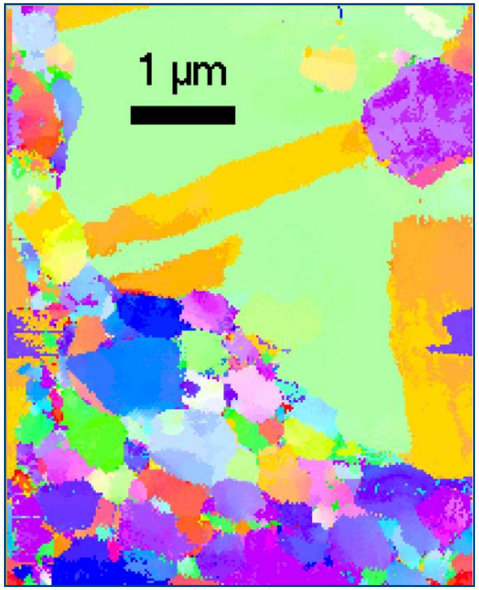

Phase ID

Texture

Inter-phase Relationships

Lattice Rotations

Strain Mapping

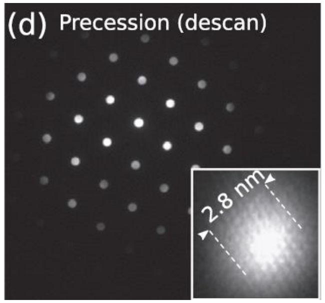

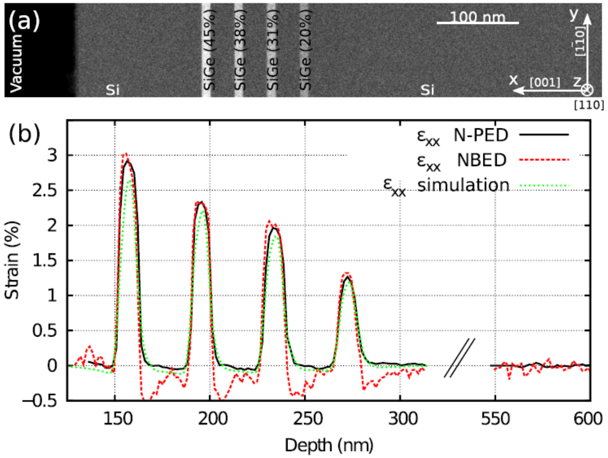

J.L. Rouviere et al
Appl. Phys. Lett.
103, 241913 (2013)

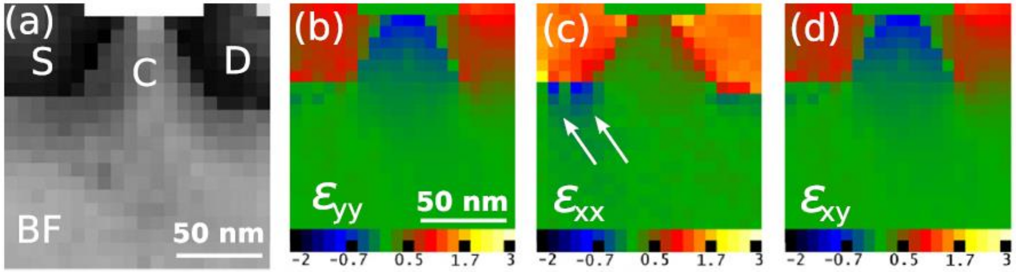

Strain (%) measured near the SiGe channel region of a transistor structure

UNIVERSITY OF CAMBRIDGE

Part II: Precession Electron Diffraction

Precession electron diffraction: a history

1937

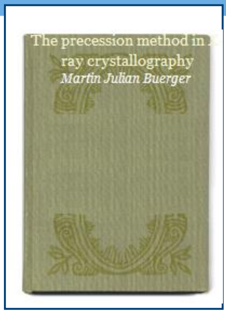

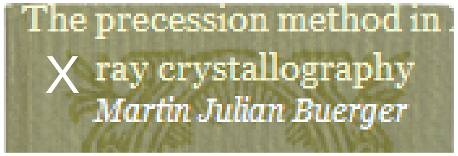

1976

Ultramicroscopy 2 (1976) 53–67

A METHOD FOR PRODUCING HOLLOW CONE ILLUMINATION ELECTRONICALLY IN THE CONVENTIONAL TRANSMISSION MICROSCOPE

William KRAKOW and Leon A. HOWLAND
Xerox Corporation, Xerox Square, W114 Rochester, N.Y. 14644, USA

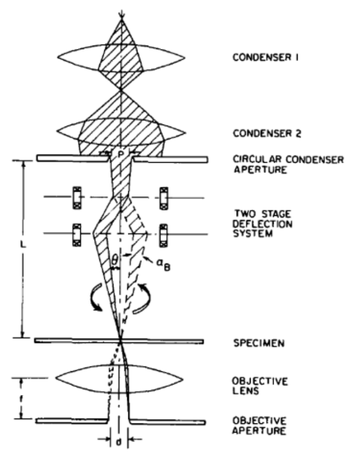

Fig. 2. Schematic diagram of ray paths for electronic hollow cone illumination.

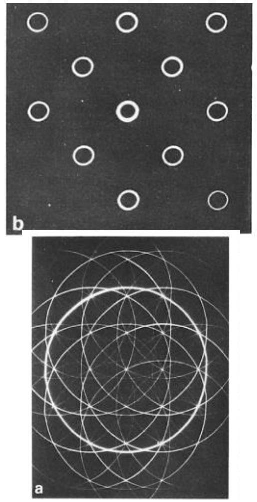

1980

Ultramicroscopy 5 (1980) 71–74

ZONE-AXIS PATTERNS FORMED BY A NEW DOUBLE-ROCKING TECHNIQUE

J.A. EADES
H.H. Wills Physics Laboratory, University of Bristol, Bristol BS8 1TL, UK

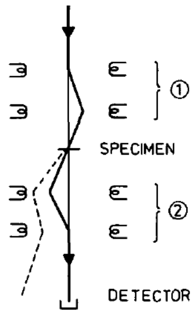

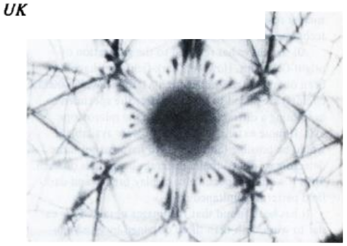

Fig. 1. Schematic diagram of the principle of the method. Two sets of coils are used: (1) the coils before the specimen are the illumination alignment coils, used for scanning in normal STEM; (2) the coils after the specimen are the imaging lens alignment coils. The solid line represents the direct beam; the dashed line represents a diffracted beam.

1970

J. Mol. Biol. (1970) **48**, 375–393

A Scanning Microscope with 5 Å Resolution

A. V. Crewe and J. Wall†
The Enrico Fermi Institute and Department c
The University of Chicago, Chicago, Ill. 6063

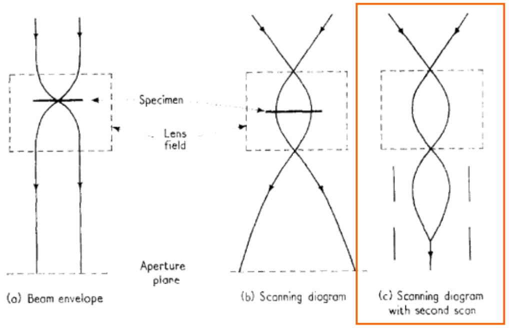

UNIVERSITY OF CAMBRIDGE

Electron analogue of Buerger's precession X-ray method

Ultramicroscopy 53 (1994) 271–282

Double conical beam-rocking system for measurement of integrated electron diffraction intensities

R. Vincent, P.A. Midgley

H.H. Wills Physics Laboratory, University of Bristol, Tyndall Avenue, Bristol BS8 1TL, UK

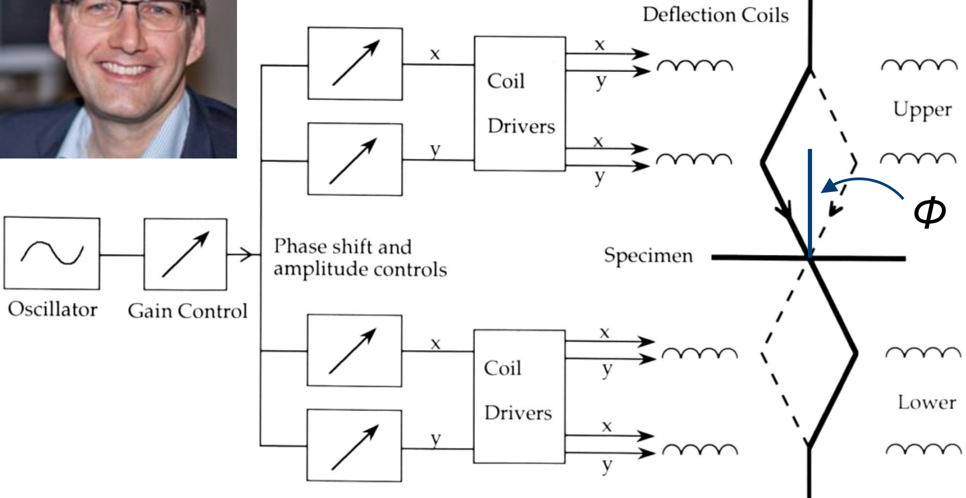

Precession angle Φ

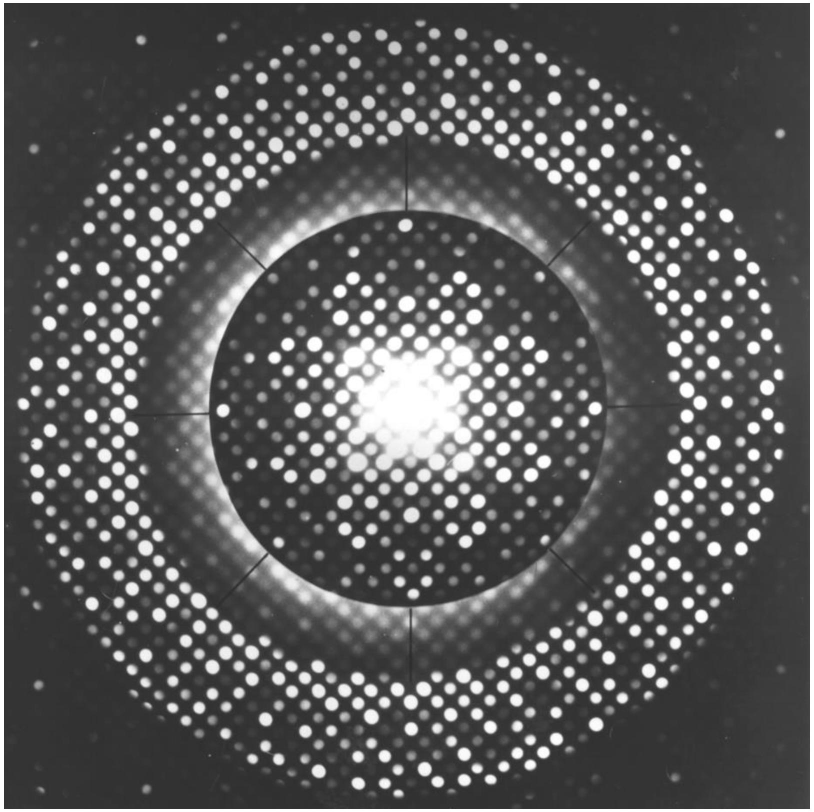

[001] $Er_2Ge_2O_7$

Zone-axis PED geometry: sample more reciprocal space

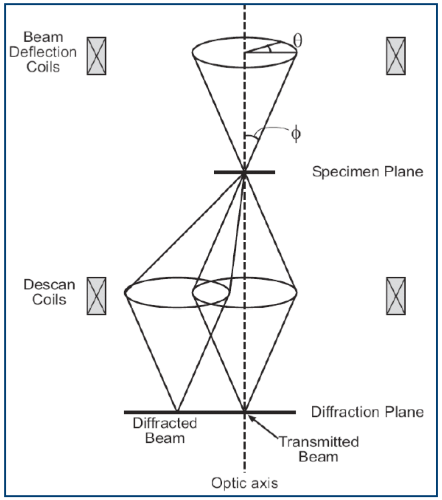

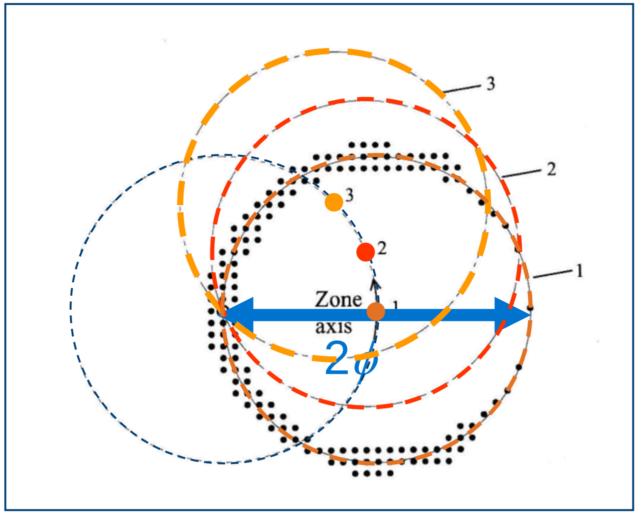

Incident beam is NEVER parallel to the zone axis – multi-beam dynamical effects minimised

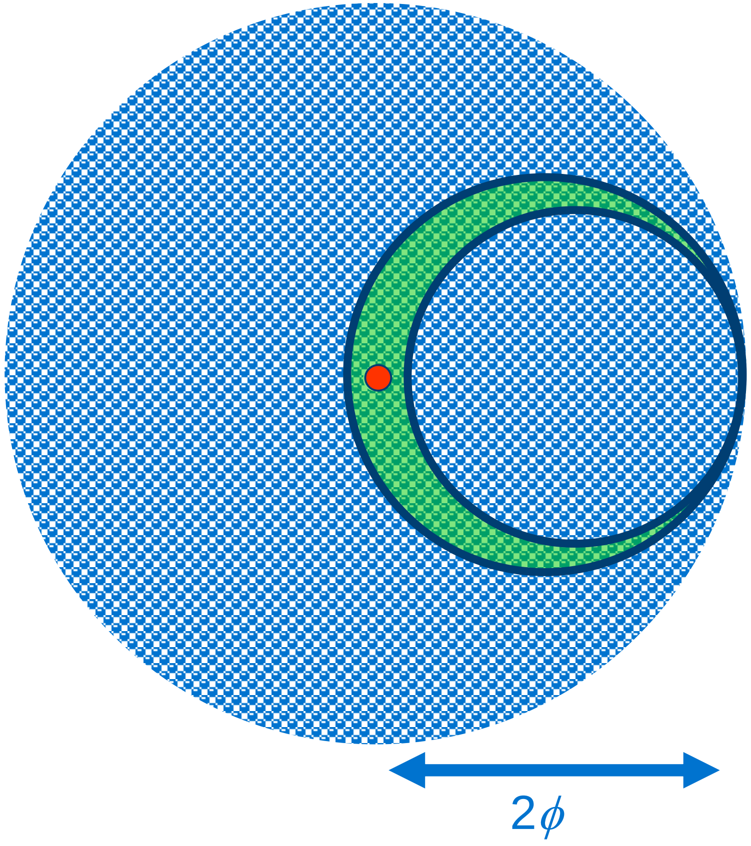

Zone-Axis Precession Electron Diffraction Geometry

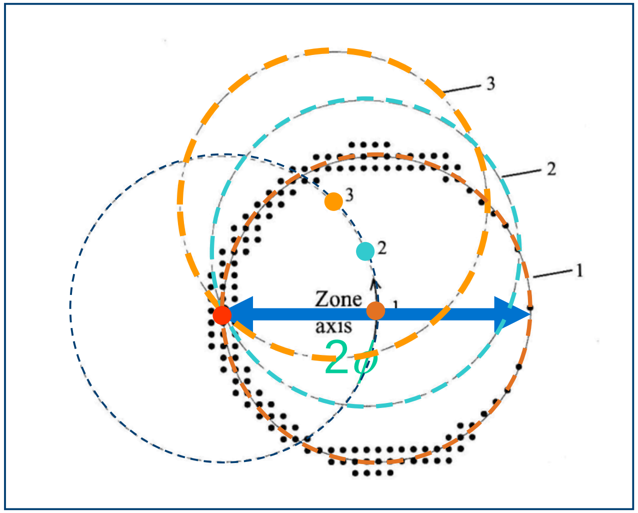

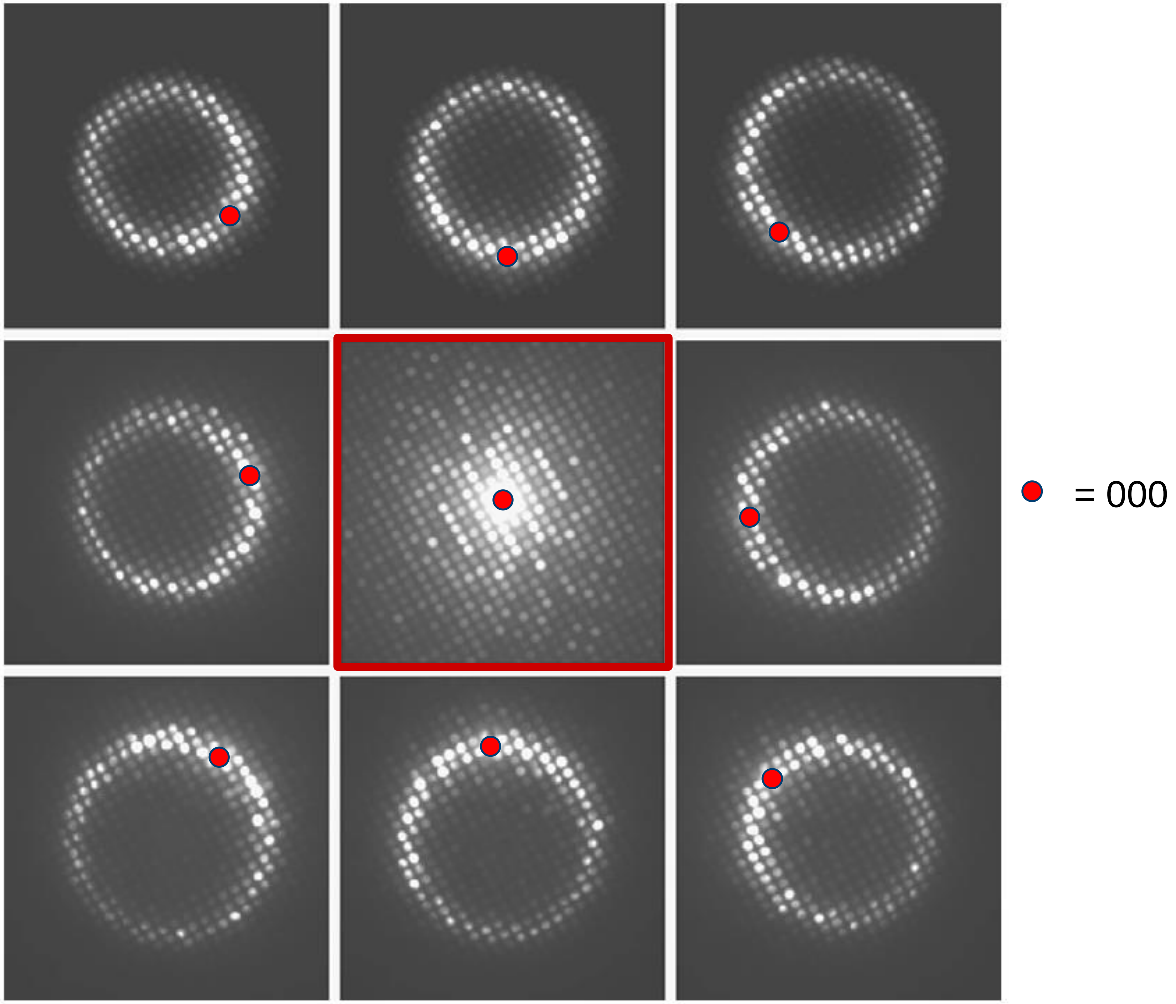

Diffraction patterns recorded from bismuth manganite.

Patterns recorded at several points around a precession circle of ϕ =1.5°.

Resultant PED pattern is sum of all off-axis patterns

Zone-axis precession electron diffraction

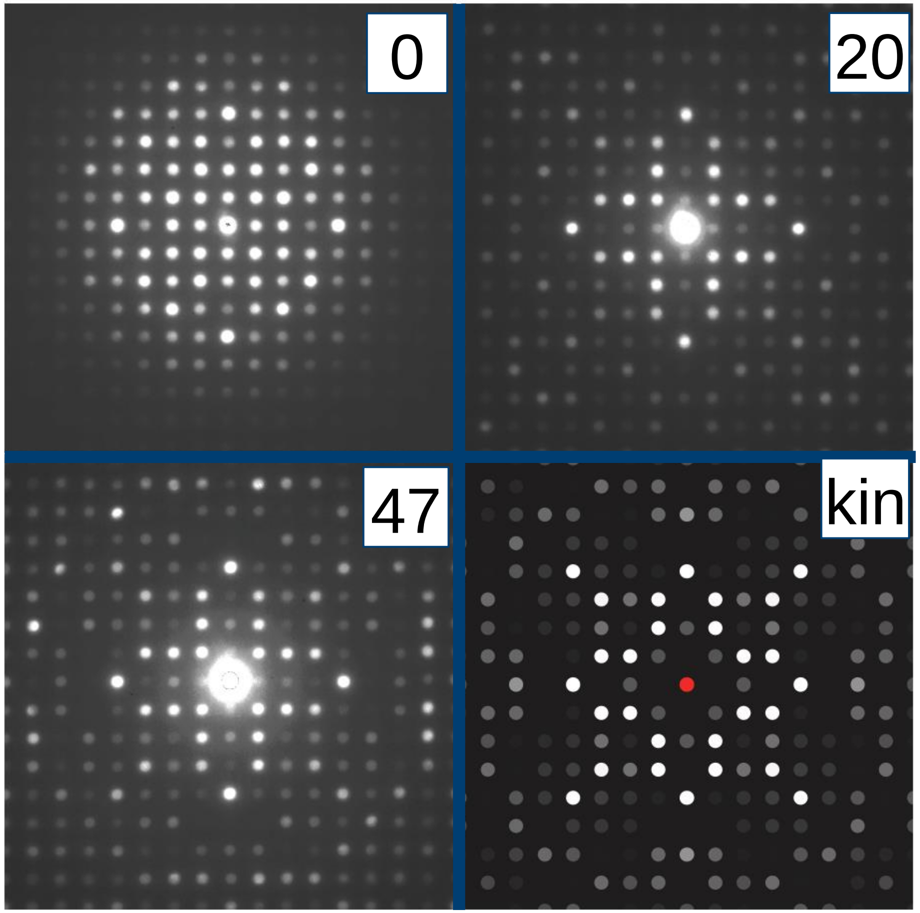

$Er_2Ge_2O_7$ With increase in precession angle, patterns look qualitatively 'more kinematical'

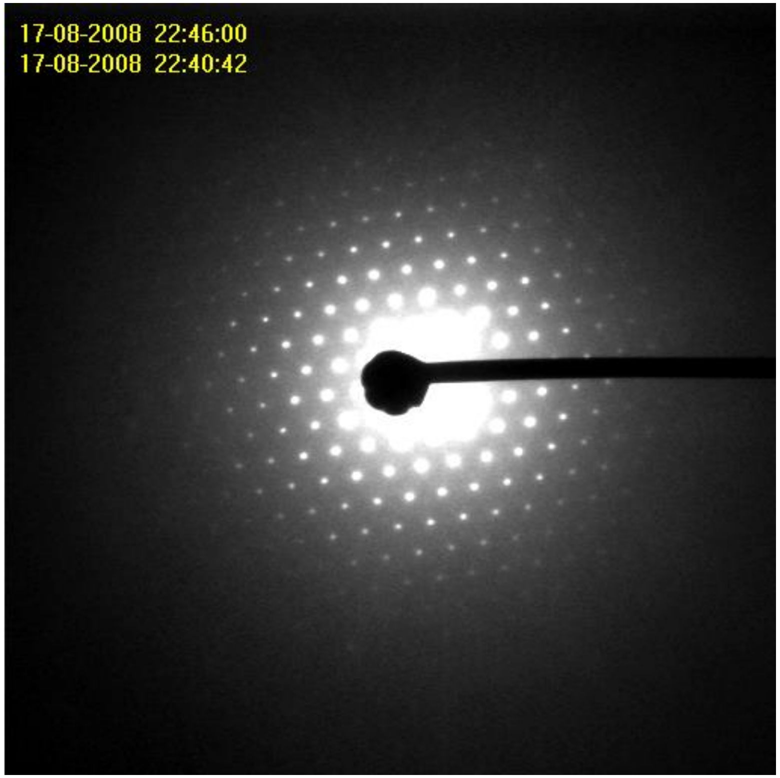

Mayenite *$Ca_{12}Al_{14}O_{33}$*

Movie courtesy of Yves Maniette (NanoMegas) – precession angle: 0 to 50 mrad

Possible to refine but very difficult to solve structures from dynamical inte

Advantages of precession electron diffraction

1. Precession – many more reflections intercepted by Ewald Sphere – large data set.
2. Diffracted intensities determined by *integrating* through Bragg condition
3. Focussed probe: $d \sim C_s \Phi^2 \alpha$
4. Reduces (sometimes!) effects of dynamical scattering → 'kinematical' intensities?

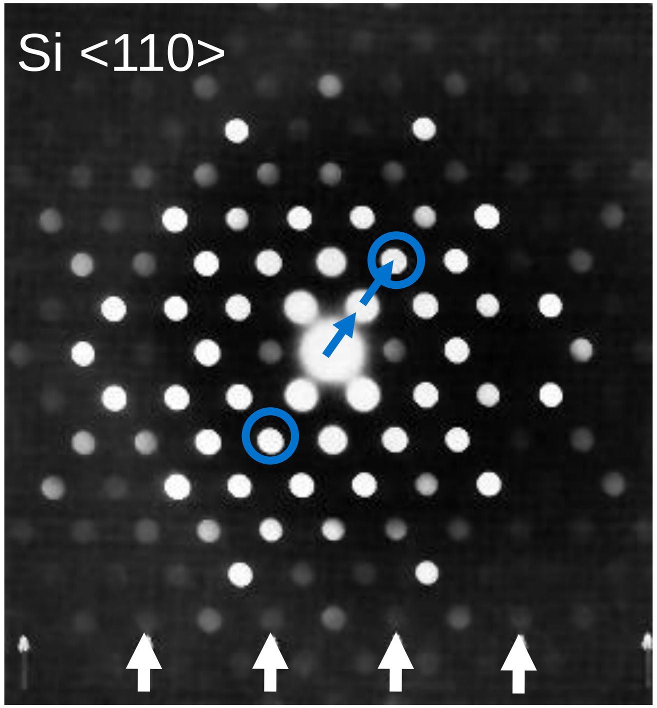

From C.S. Own PhD Thesis

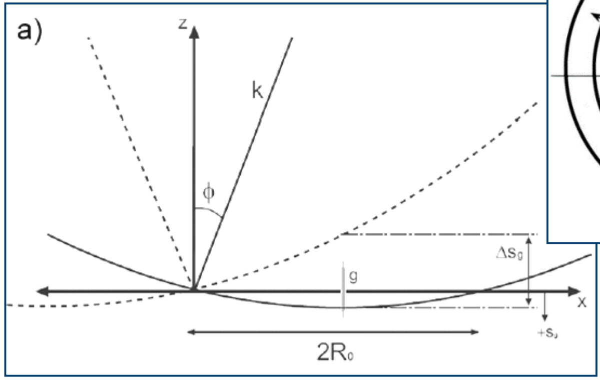

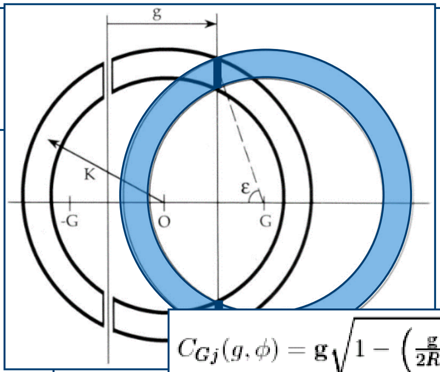

$$C_{Gj}(g,\phi) = \mathbf{g}\sqrt{1-\left(\frac{\mathbf{g}}{2R_0}\right)}$$

geometric correction

Rows of reflections arrowed should be absent
($F_{hkl} = 0$ for $h+k+l = 4n+2$)

Reflections present along $\{hhh\}$

Intensities of kinematically-forbidden reflections

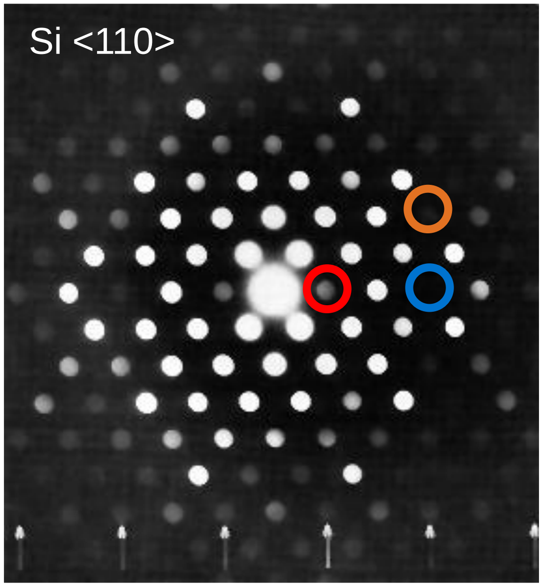

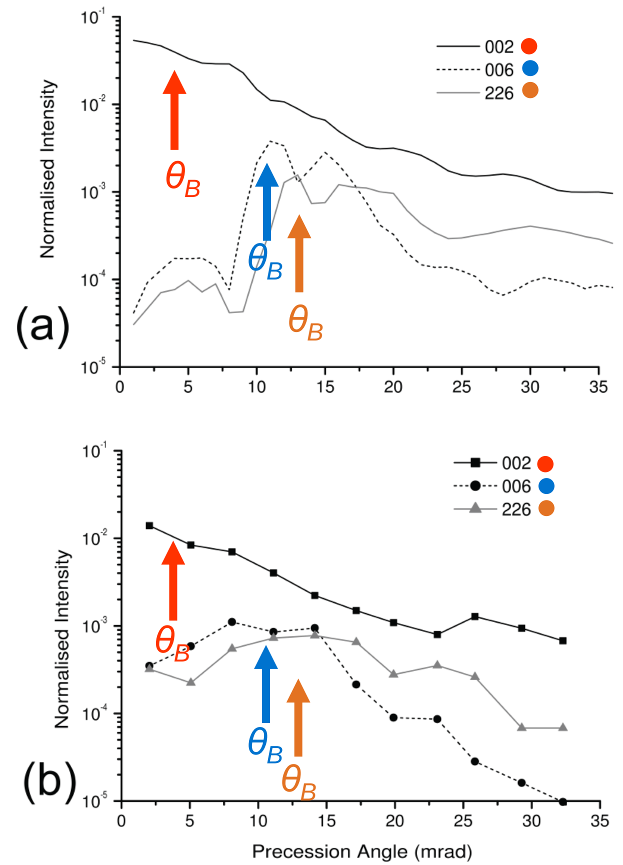

Simulation

Experiment

Intensity vs precession angle for kinematically-forbidden reflections

Precession angle and LACBED

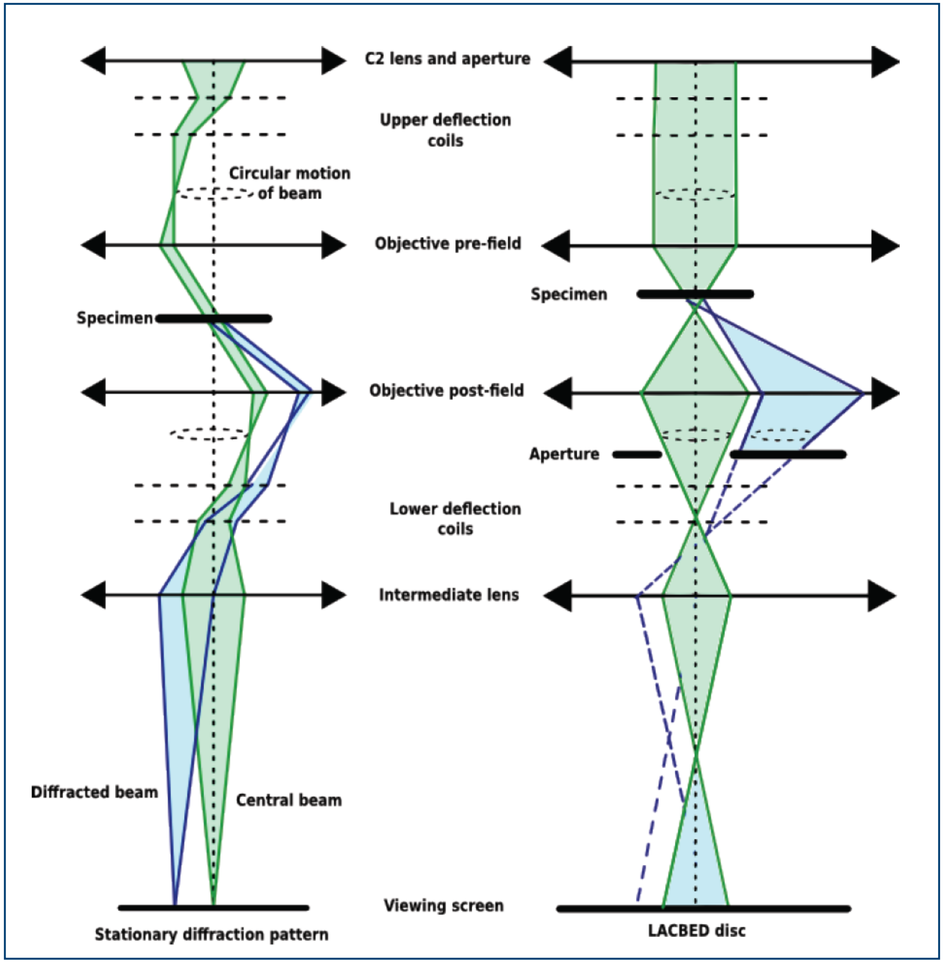

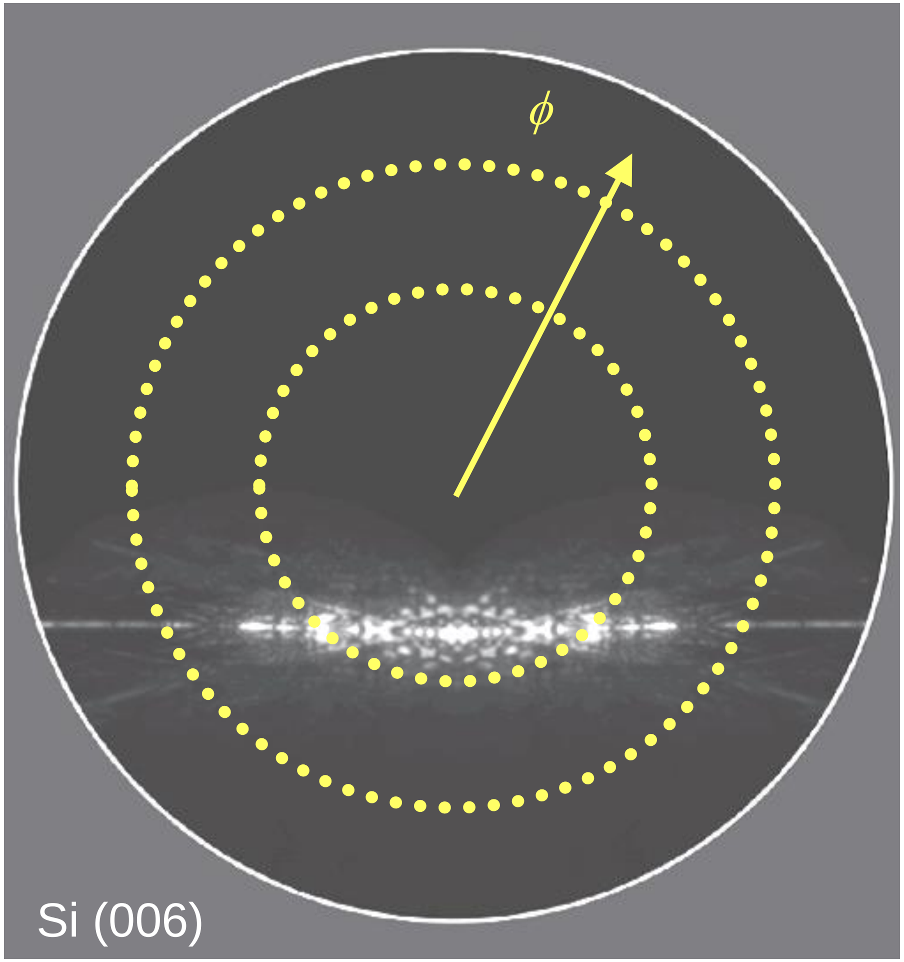

Kinematically forbidden reflectios - 222

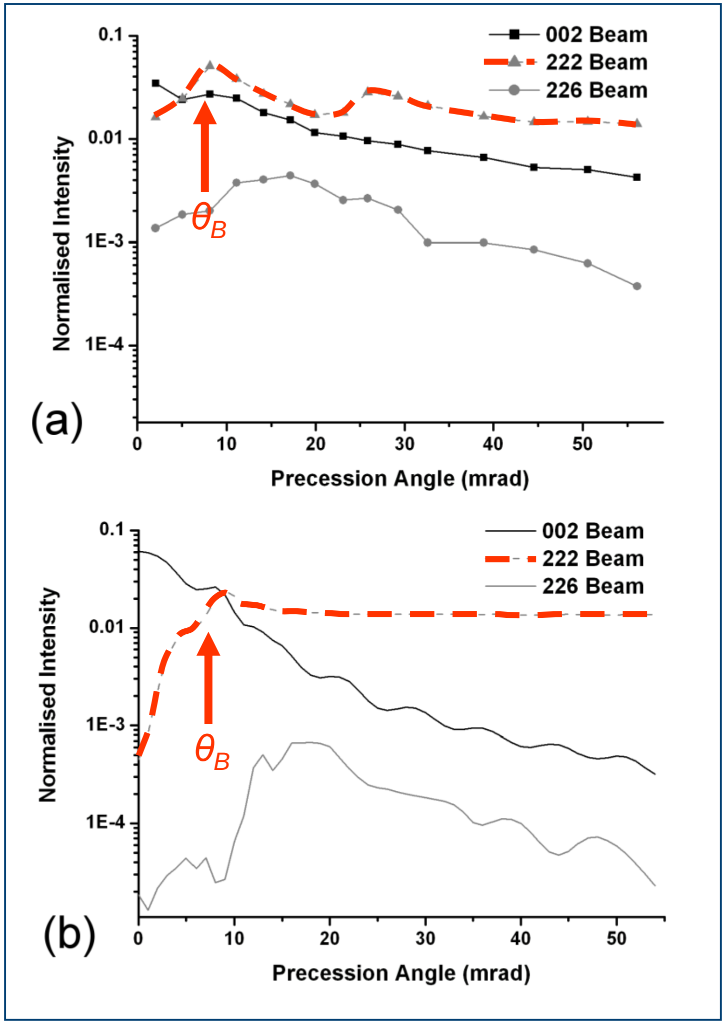

Experiment

Simulation

Precession angle and LACBED

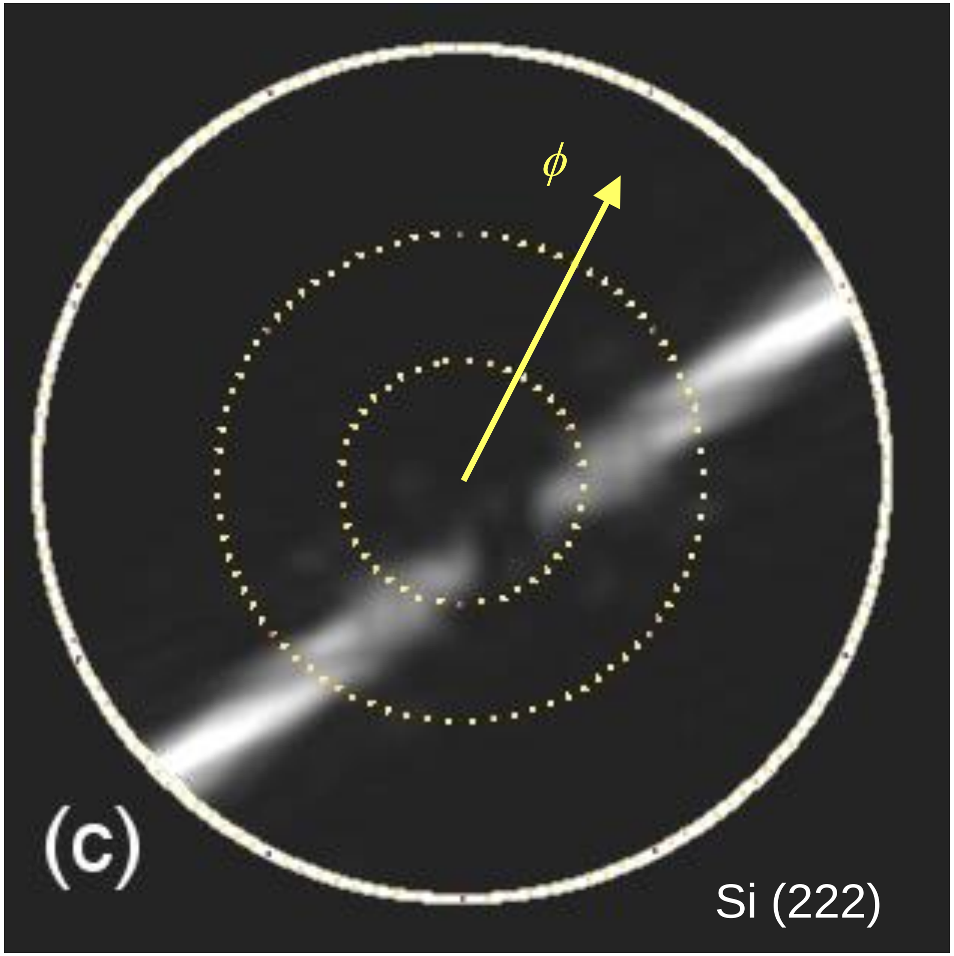

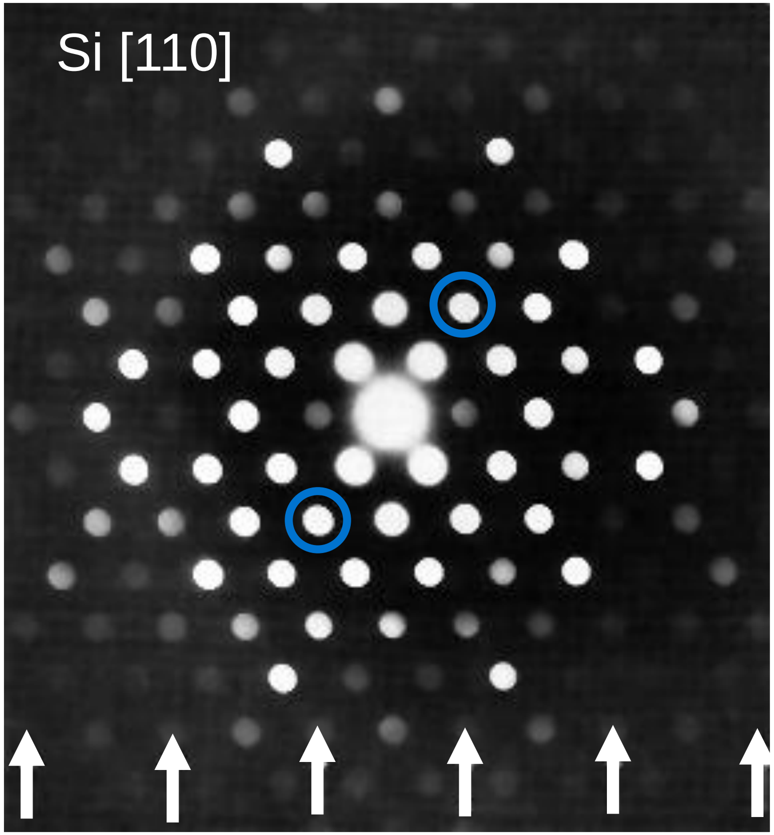

Solving crystal structures: ZOLZ

[001] $Er_2Ge_2O_7$

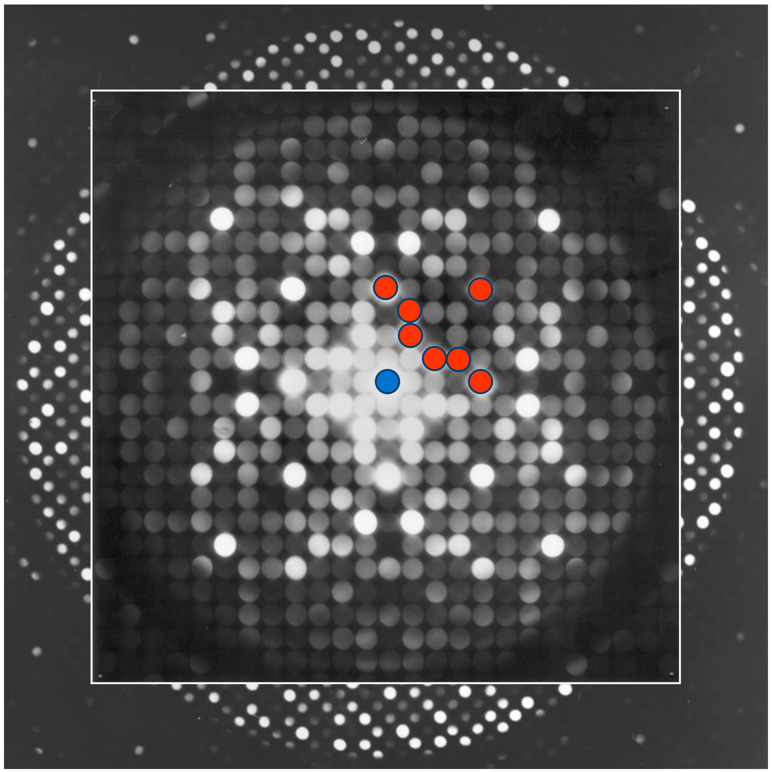

Direct Methods

Probabilistic methods to allow guesses as to correct phases of structure factors.

Space group symmetry (projection) allows some **strong** *hk*0 reflections to be assigned phases.

Phase triplets: $\phi(-\mathbf{h}) + \phi(\mathbf{k}) + \phi(\mathbf{h}-\mathbf{k}) \approx 0$

The rest assumed initially random but then 'refined' to give best consistent set of phases.

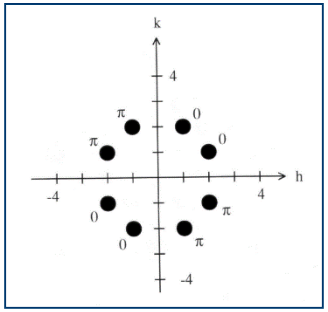

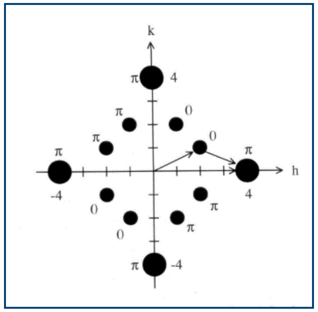

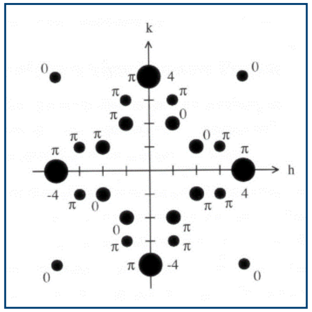

Structure ‘solutions’ using ZOLZ & direct methods

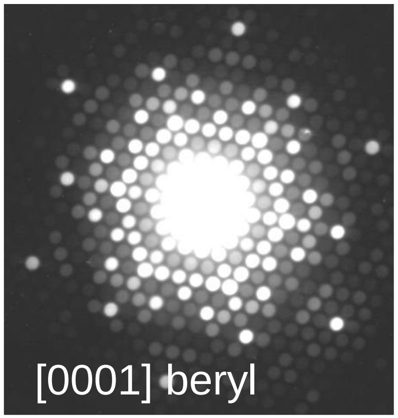

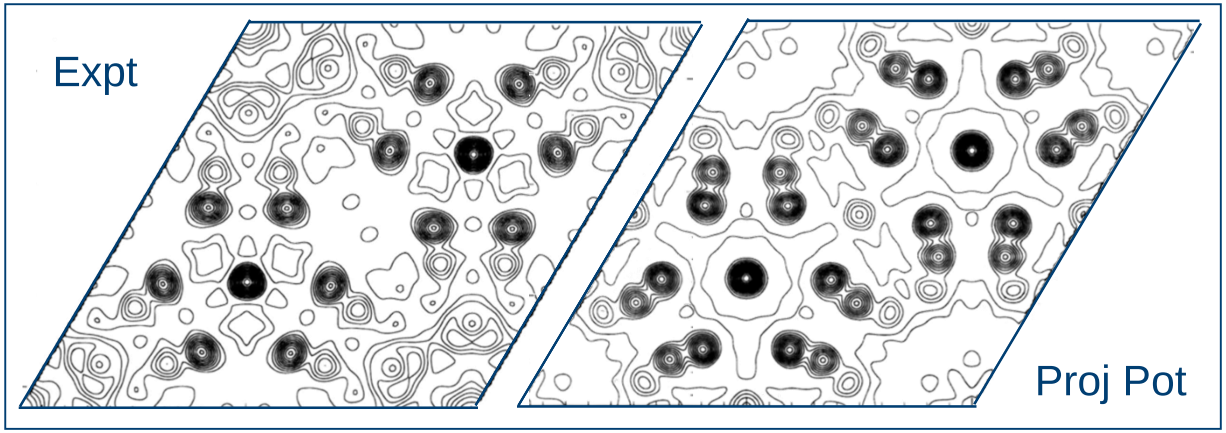

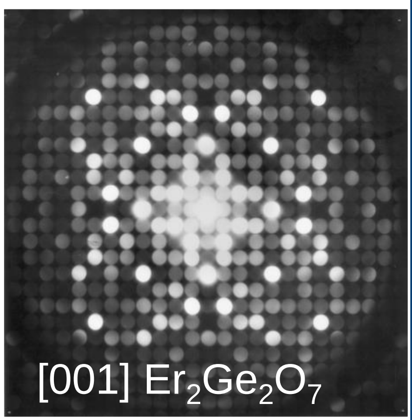

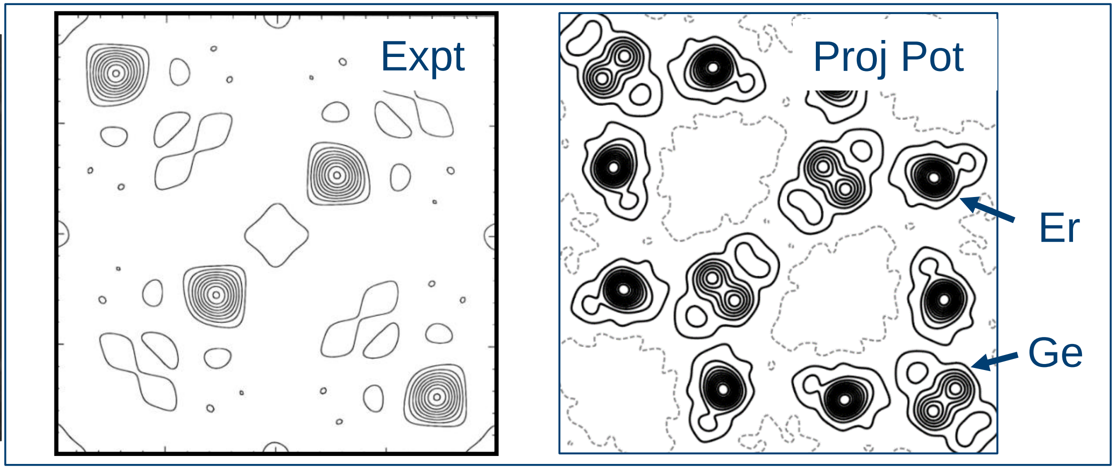

So how akinematical are PED intensities?

For ***<u>kinematical</u>*** intensities:

and the intensity is independent of other reflections

$$I_g \propto \left|F_g\right|^2$$

<u>Dynamical</u> diffraction: - diffracted beams interfere and resultant intensity depends on structure factors (phases) of all beams.

$$I_g = f(F_g, F_h, F_i, F_j ....)$$

If intensities are kinematical, they will be <u>insensitive</u> to the phases of all other structure factors.

Many possible structures can produce the same kinematical diffraction intensities (although not all structures are reasonable).

Can scramble phases of Fourier components of projected potential to create a model of such a structure.

Phase scrambling: testing for kinematic behaviour

Each *homometric* structure will give the <u>same kinematical</u> diffraction pattern (structure factor moduli) but <u>different dynamical</u> patterns

Original
(Si <110>)

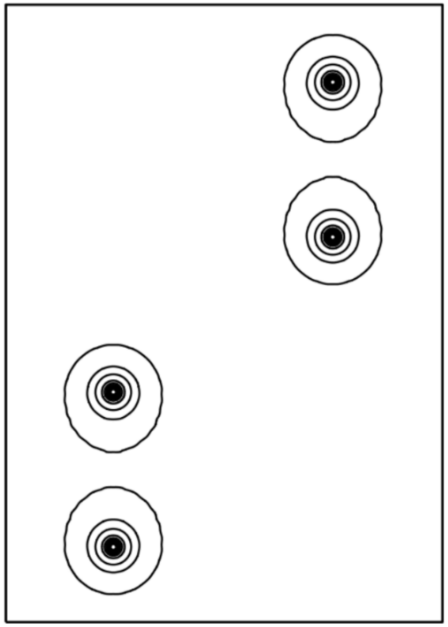

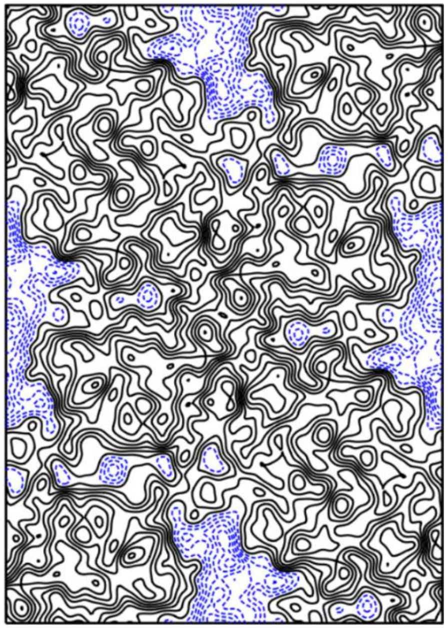

Blue indicates negative potential

Altered
(Phases Scrambled)

If precession make intensities 'more kinematical' then the diffracted intensities from these two structures should converge to being the same at sufficiently high precession angles.

Phase scrambling – dynamical multislice calculation

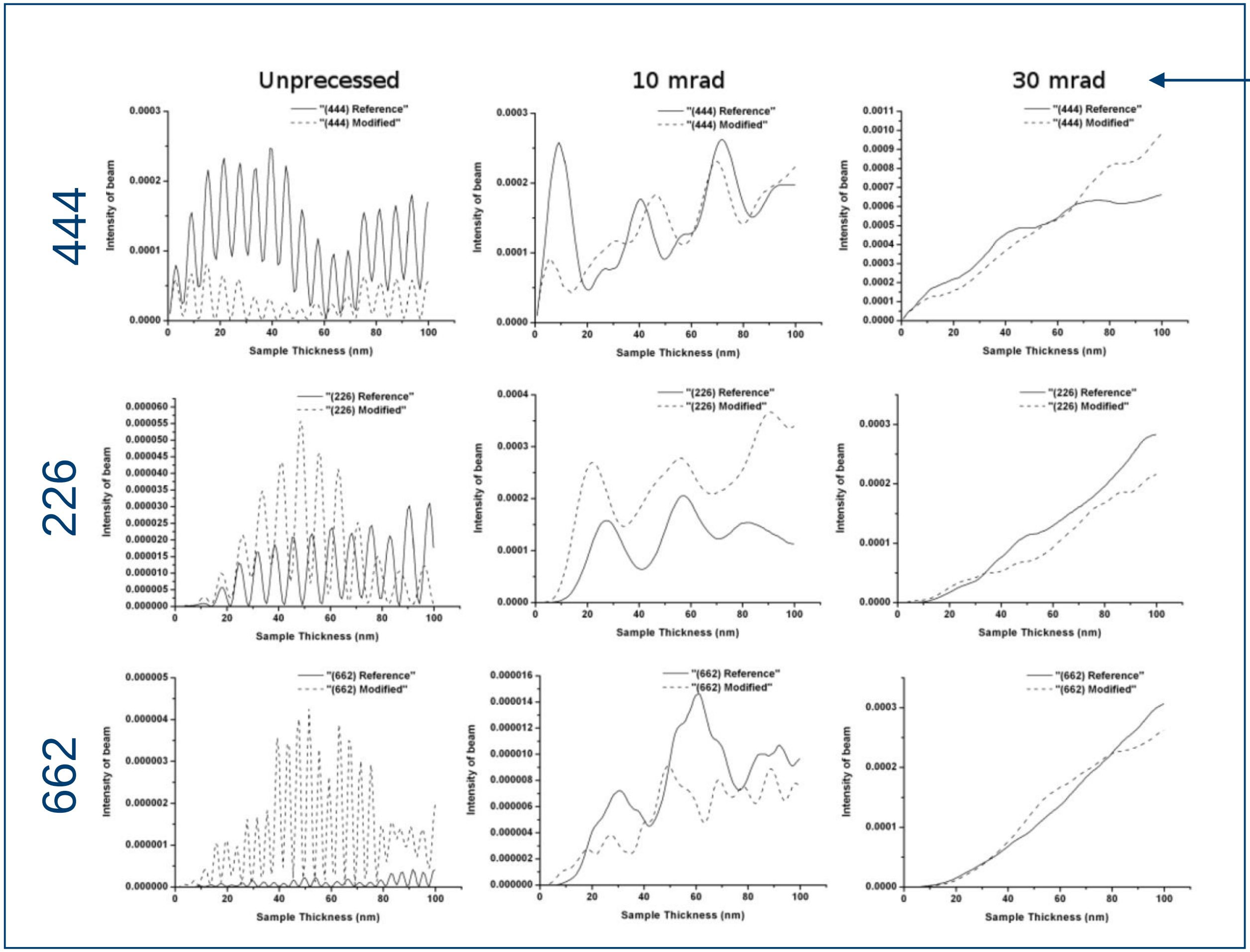

Precession Angle

Solid line original

Dashed line altered

Simulated (multislice) intensities of (a) 444, (b) 226 and (c) 662 for Si [110]

Phases Scrambling – multislice Si [110] @ 300kV

444

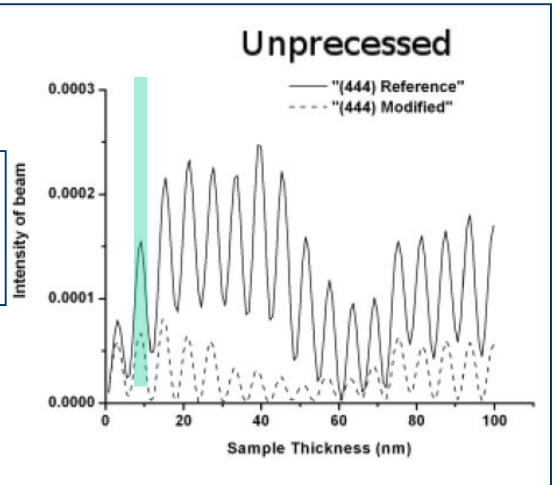

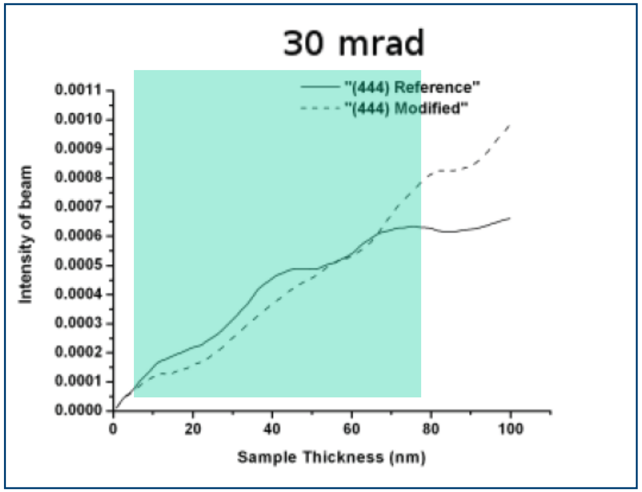

004

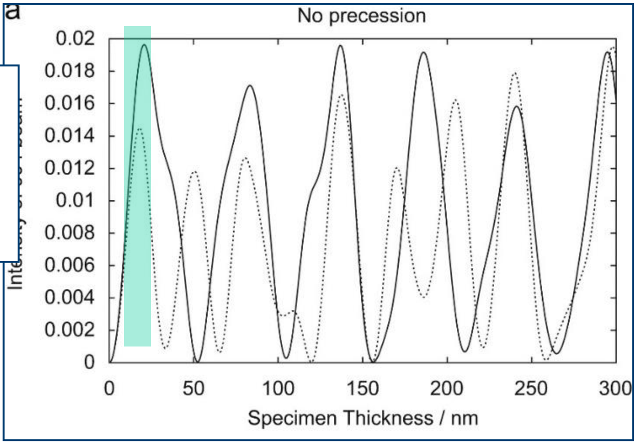

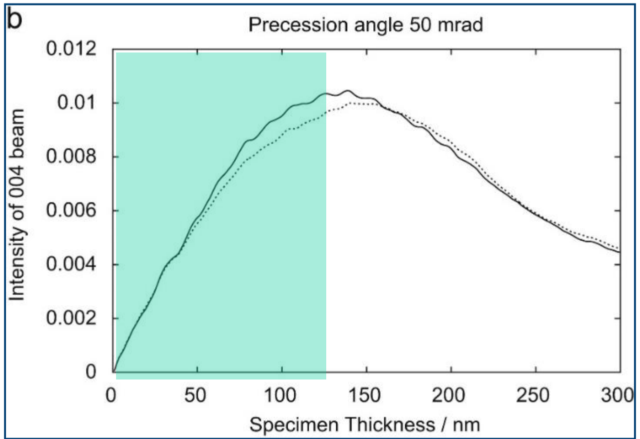

Solid line
original

Dashed line
altered

Intensity of phase-altered reflections

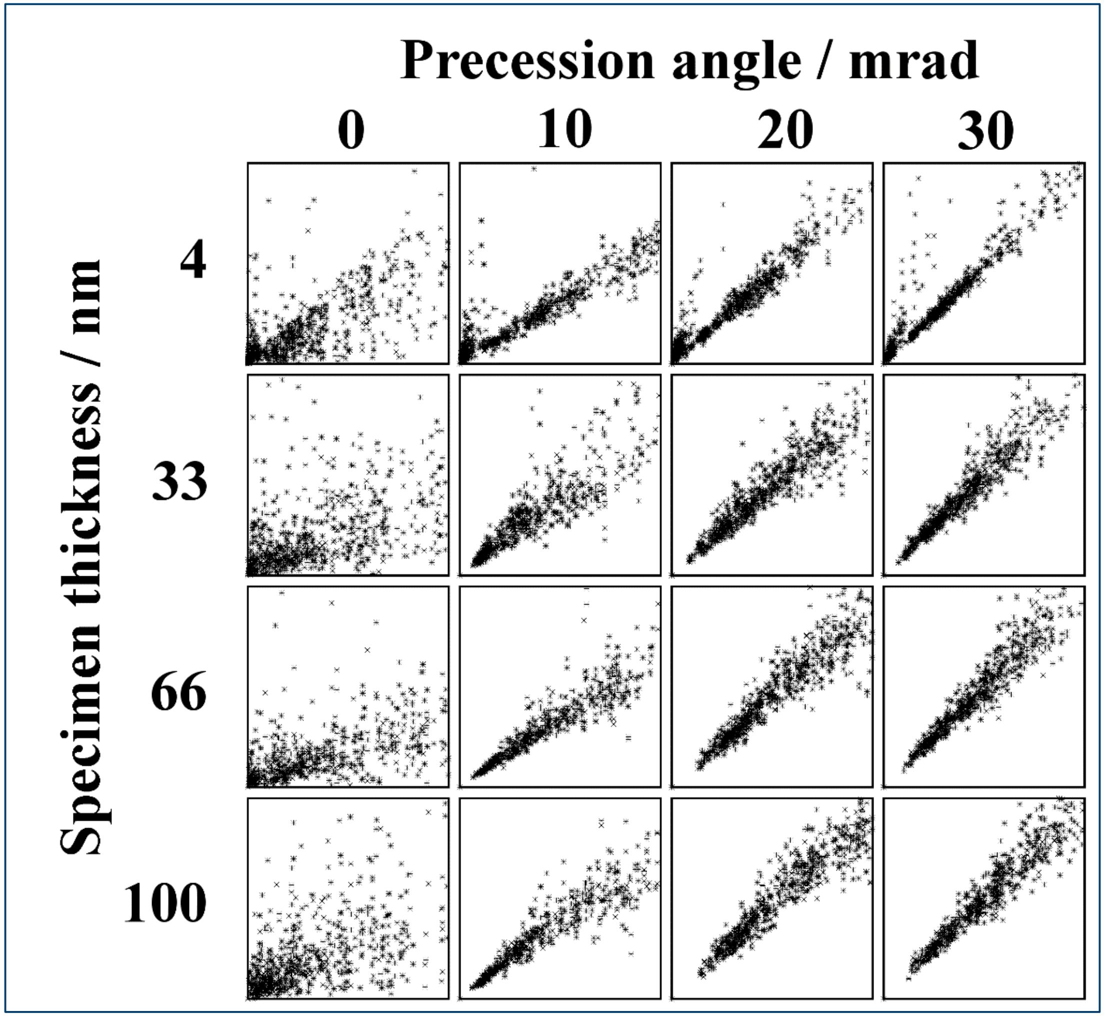

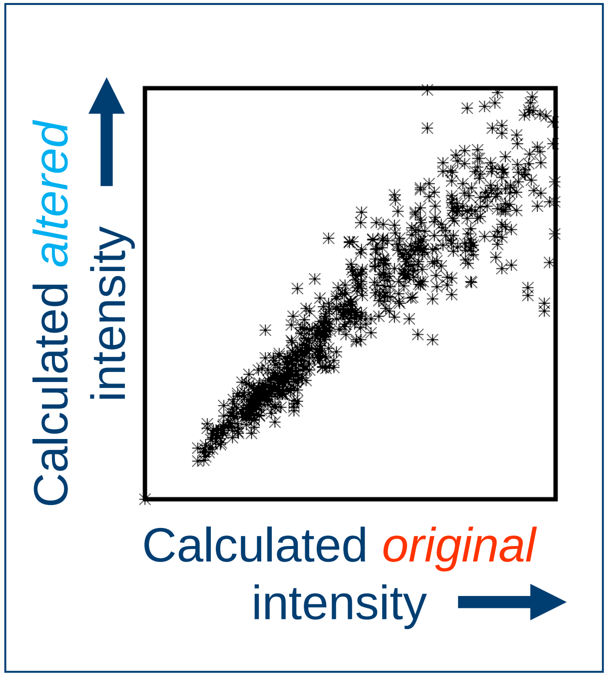

If intensities correlated then I_g independent of phases and ∴ 'kinematic'

So why didn't EGO work?

Structure refinement – ‘how good’ is our solution?

Conventional refinement techniques comparing experimental intensities to kinematical ones the refinement value is poor.

$$R_1 = \frac{\sum_{\mathbf{h}} \left(|F_{\mathbf{h}}|_{\text{obs}} - k\,|F_{\mathbf{h}}|_{\text{calc}} \right)}{\sum_{\mathbf{h}} |F_{\mathbf{h}}|_{\text{obs}}},$$

Typically our R_1 values are 30-50% (X-ray refinements are often a few%)

Why so bad?! Data is not kinematical – We are comparing apples and pears!!

But data can’t be so bad because we’re getting good structure solutions!

New developments can help overcome challenges:

Iterative structure solution algorithms (charge flipping) – better solutions

Acquire 3D data – better constrained

Dynamical refinement – better refined

Charge Flipping: Structure solution with constraints
(Oszlanyi and Suto, Acta Cryst A 2004)

1. Real space: *positivity*
2. Reciprocal space: *diffracted intensities*

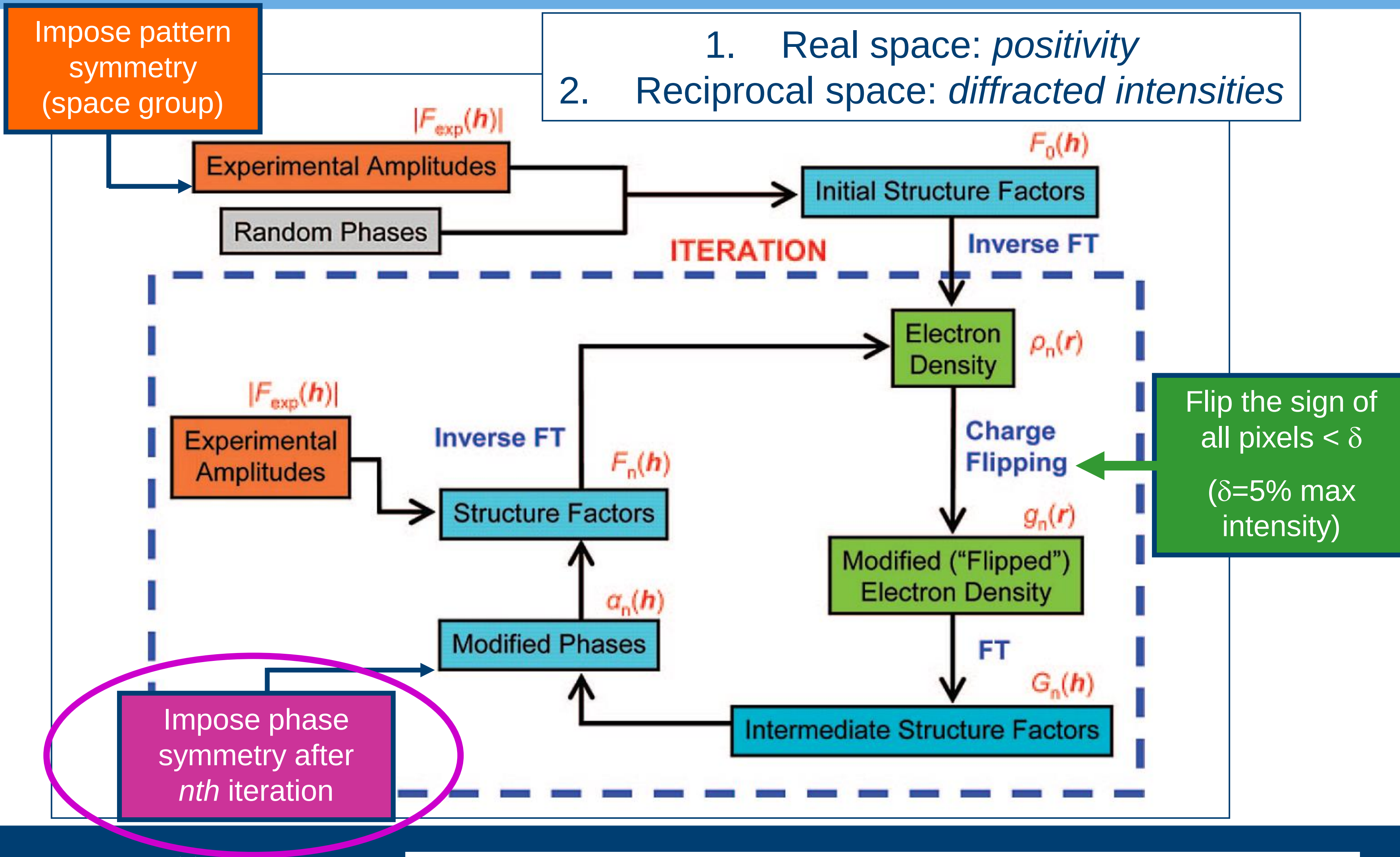

A Eggeman, T White and P Midgley *Acta Cryst A* (2009) 65 120

Structure 'solutions' using ZOLZ & charge flipping

40-iterations with symmetry imposition

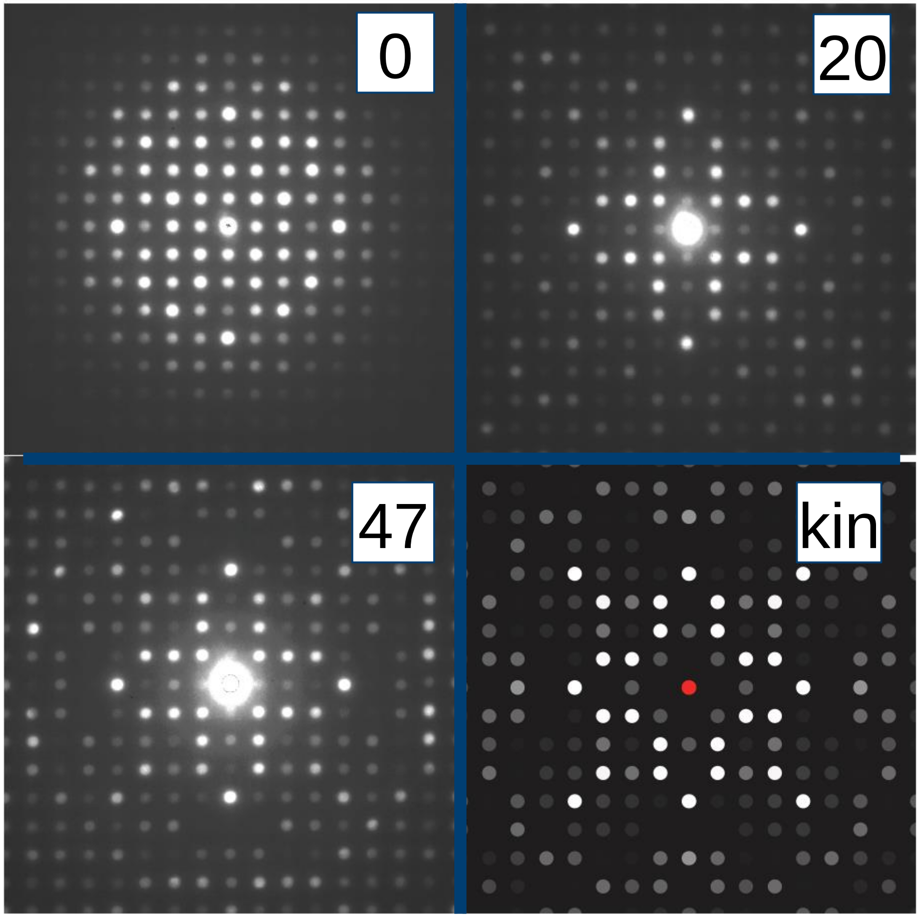

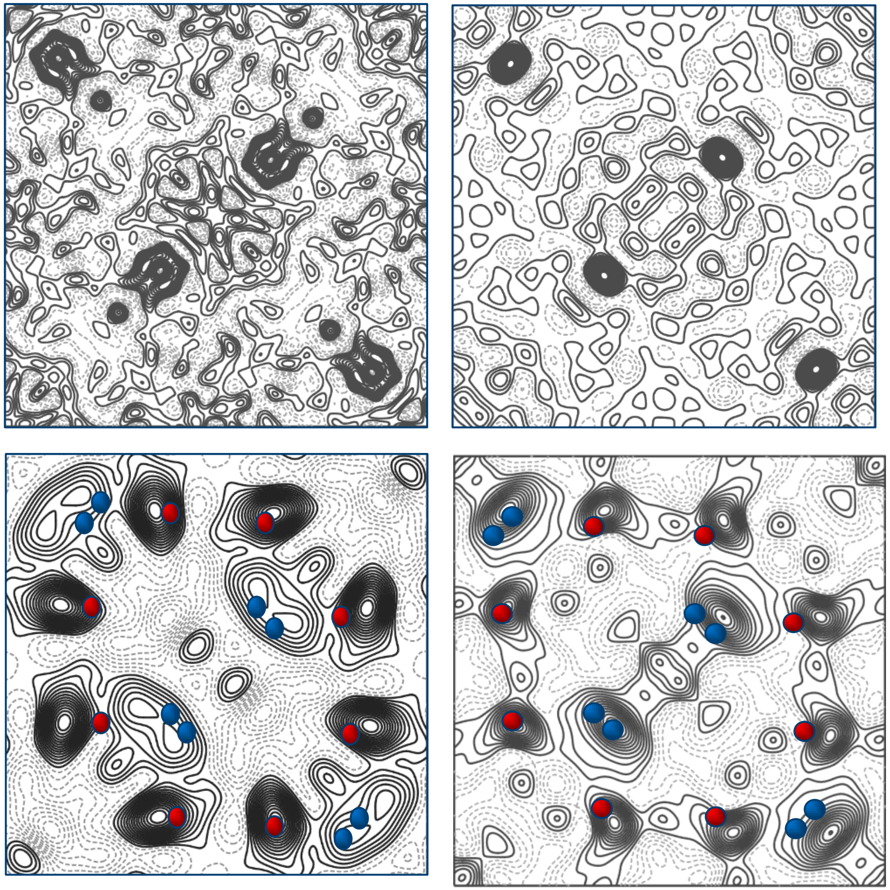

UNIVERSITY OF CAMBRIDGE

Automated Diffraction Tomography

'Diffraction Tomography' (2008) – acquiring PED patterns about a 'random' single axis → 3D data

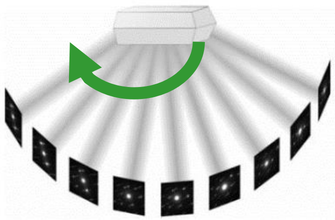

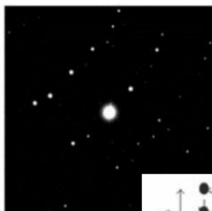

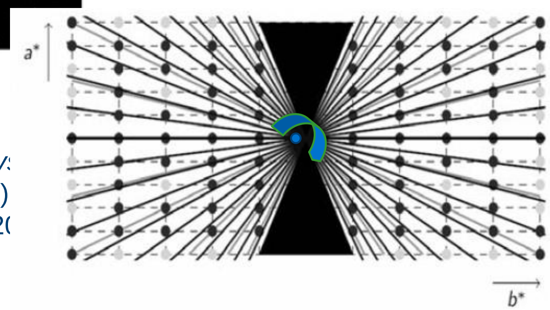

U. Kolb, E. Mugnaioli, and T. E. Gorelik *Cry*
Technol. 46, No. 6, 542 – 554 (2011)
Mugnaioli, E., Gorelick, T., & Kolb, U. (2(
Ultramicroscopy, 109, 758–765.

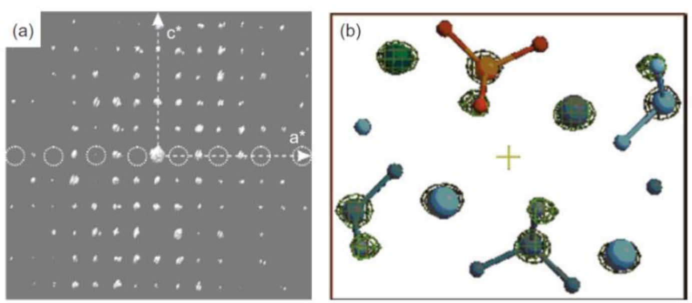

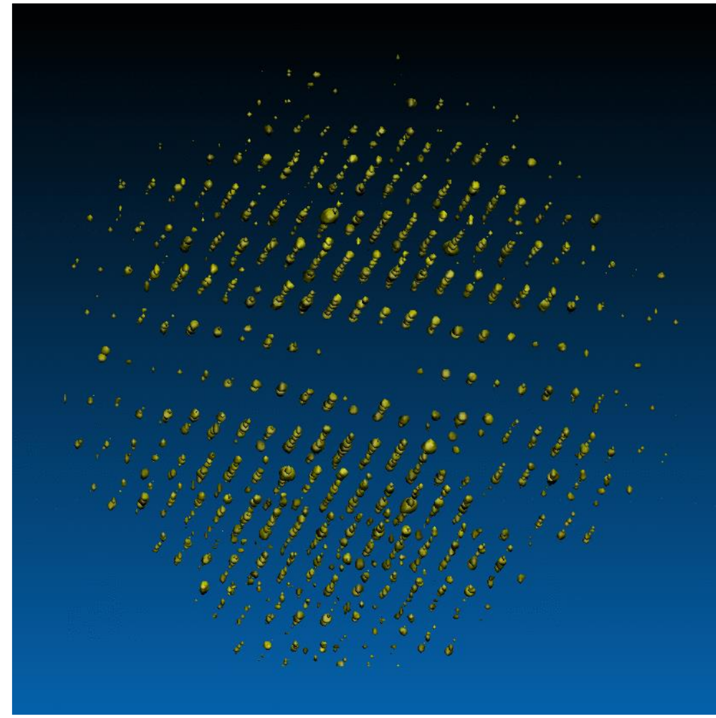

3D data from $Mg_3Al(OH)_3Si_2O_7$ synthesized at 6.5 GPa, 700 C

Movie courtesy of Mauro Gemmi (IIT) Pisa

ISTITUTO ITALIANO DI TECNOLOGIA

Dynamical Refinement

L. Palatinus et al *Acta Cryst.* (2013) A69, 171–188

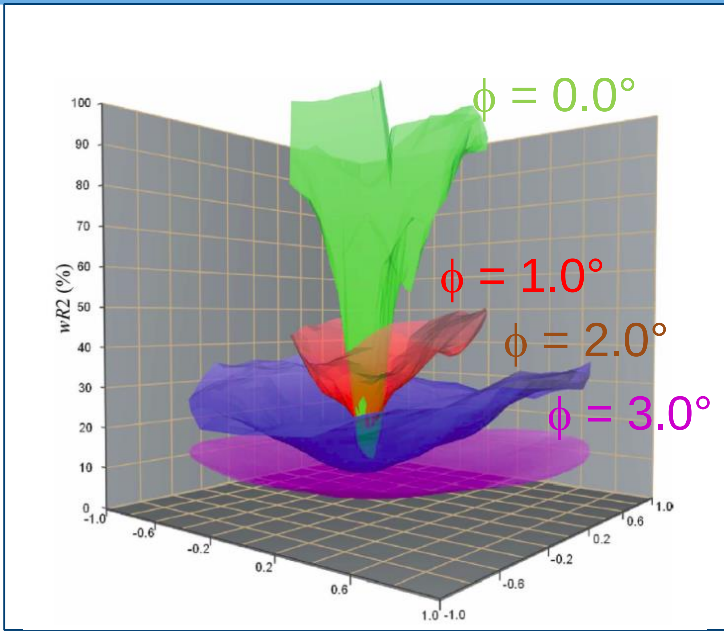

Table 16
Refinement of all permitted structure parameters of the orthopyroxene structure against the data set opht1p2.4.

Maximum and average distance mean the distances from the reference structure refined against X-ray diffraction data.

	Kinematical	Two-beam	Dynamical
$wR2$, $R2$, $R1$ (%)	15.80, 20.63, 30.61	15.69, 19.49, 28.54	5.45, 7.48, 11.25
Maximum $U_{\rm iso}$ (Å^2)	0.0886	0.1794	0.0581
Minimum $U_{\rm iso}$ (Å^2)	−0.0099	−0.0164	−0.0085
Maximum distance (Å)	0.302	0.146	0.093
Total average distance (Å)	0.122	0.106	0.048
Average distance of cations (Å)	0.044	0.108	0.050
Average distance of O atoms (Å)	0.175	0.105	0.047
occ(Fe1)	0.571	0.413	0.134
occ(Fe2)	1.094	1.278	0.436

e.g. $R1$ (kin) 30.61% → 11.25% (dyn)

$$wR2 = \left[\frac{\sum w_{\mathbf{g}}\left(I_{\mathbf{g}}^{\rm o} - I_{\mathbf{g}}^{\rm c}\right)^2}{\sum w_{\mathbf{g}}(I_{\mathbf{g}}^{\rm o})^2}\right]^{1/2},$$

$$R2 = \frac{\sum\left|I_{\mathbf{g}}^{\rm o} - I_{\mathbf{g}}^{\rm c}\right|}{\sum\left|I_{\mathbf{g}}^{\rm o}\right|},$$

$$R1 = \frac{\sum\left|(I_{\mathbf{g}}^{\rm o})^{1/2} - (I_{\mathbf{g}}^{\rm c})^{1/2}\right|}{\sum(I_{\mathbf{g}}^{\rm o})^{1/2}}.$$

Sample orientation and thickness required accurately for dynamical refinement but not for kinematical refinement.

For dynamical refinement with PED the sample orientation and thickness is not needed quite so accurately.

Summary

1. PED gives more reflections and with intensities integrated through the Bragg condition.

2. PED intensities are <u>not</u> kinematical but, with sufficiently high precession angle, behave in some kinematic-like ways.

3. PED reduces sensitivity to orientation and thickness. Pragmatically this is often quite useful.

4. *Ab-initio* structure solution – best achieve with precession electron diffraction (PED).

5. 3D data & dynamical refinement is now the ‘gold standard’

UNIVERSITY OF CAMBRIDGE

Part III: Experimental Aspects of PED

PED optical configuration

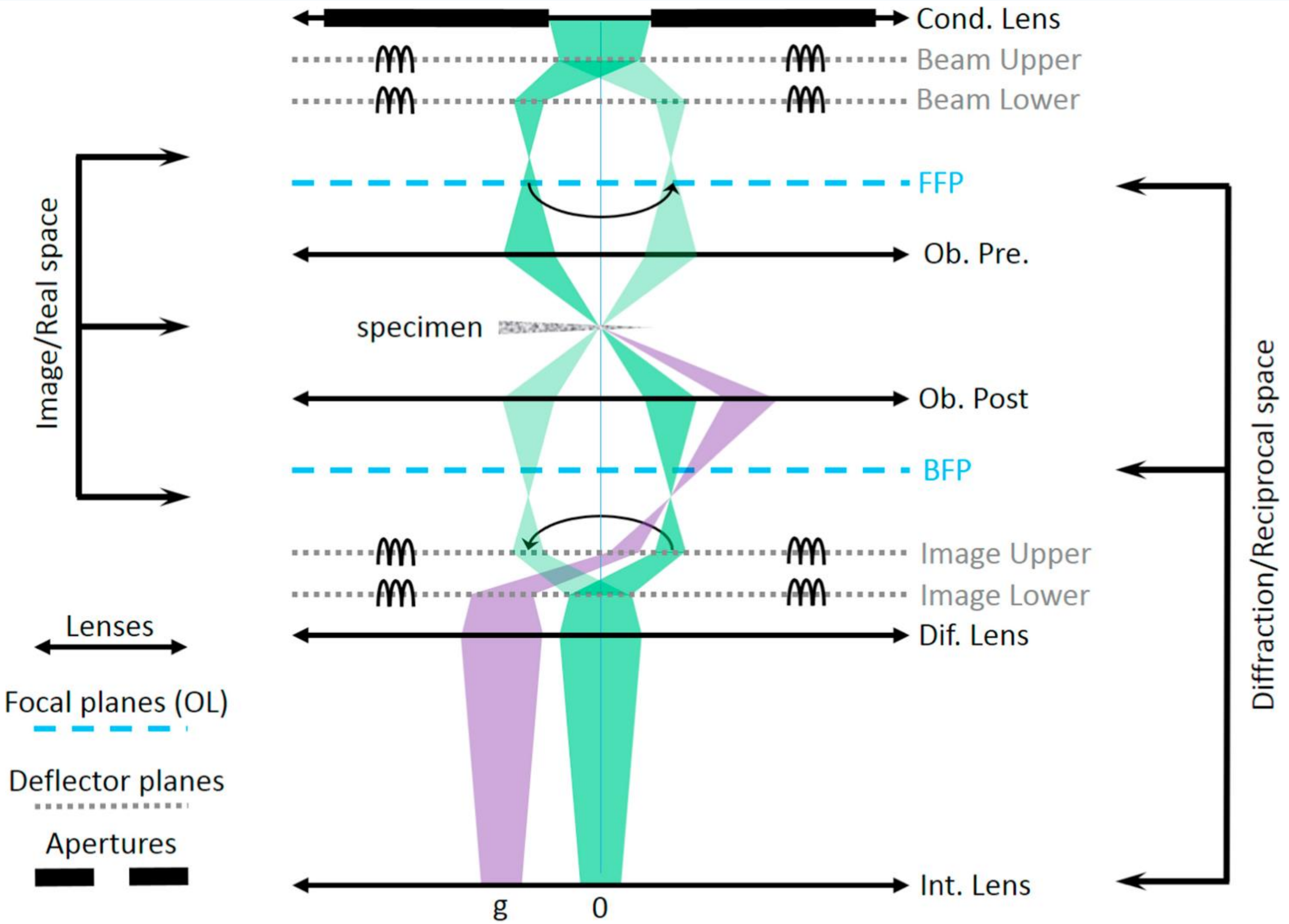

PED alignment

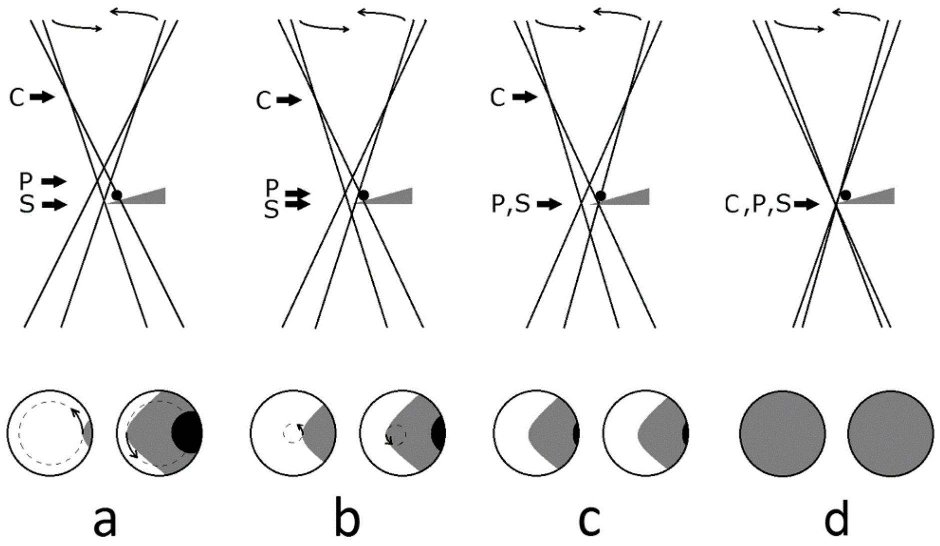

Image of the probe unreliable due to lens aberrations – use the shadow image in the Ronchigram.

Need to bring pivot point plane, condenser focal plane, and specimen plane into coincidence.

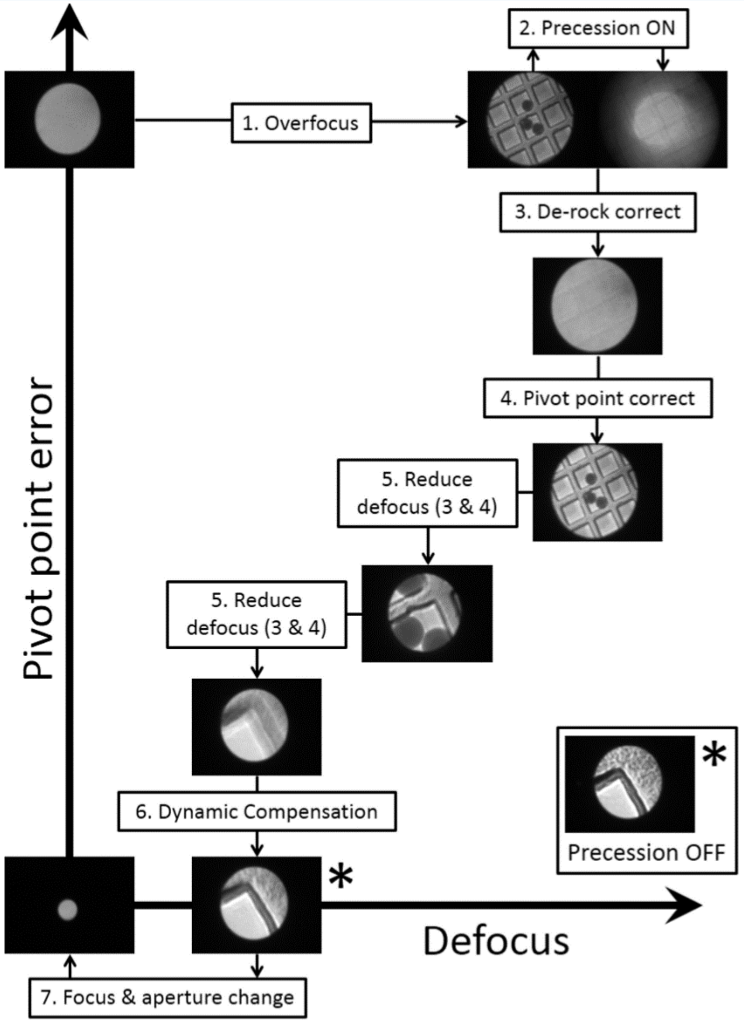

Lens Aberrations & PED probe size

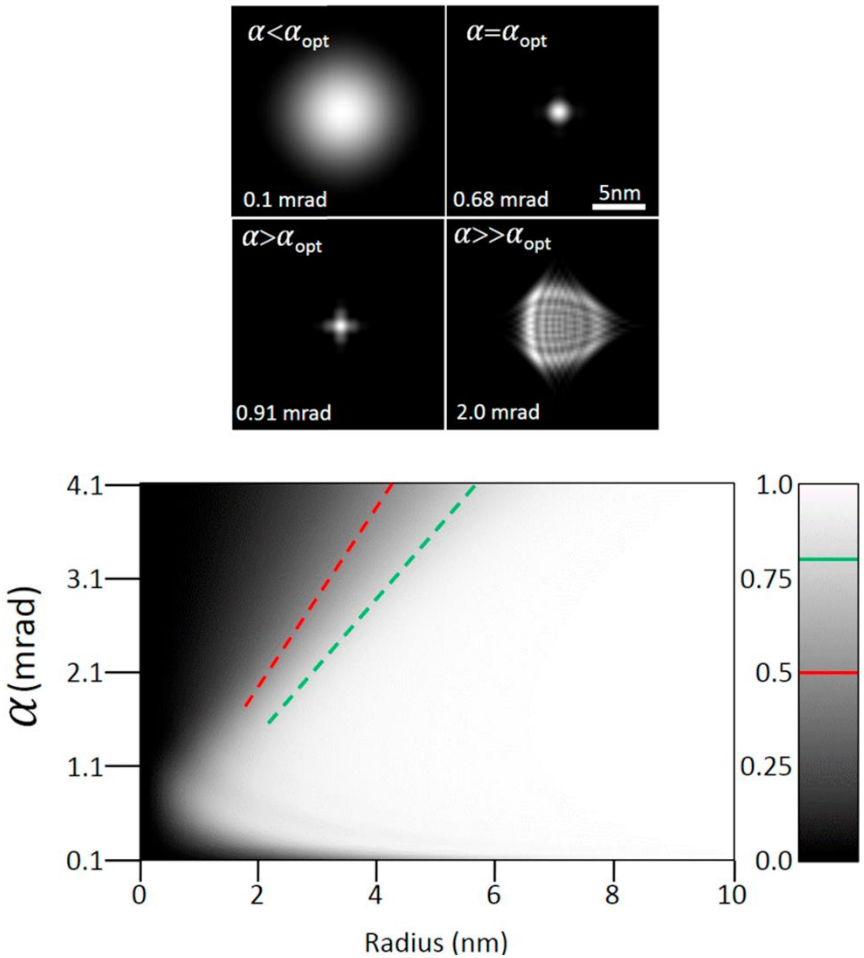

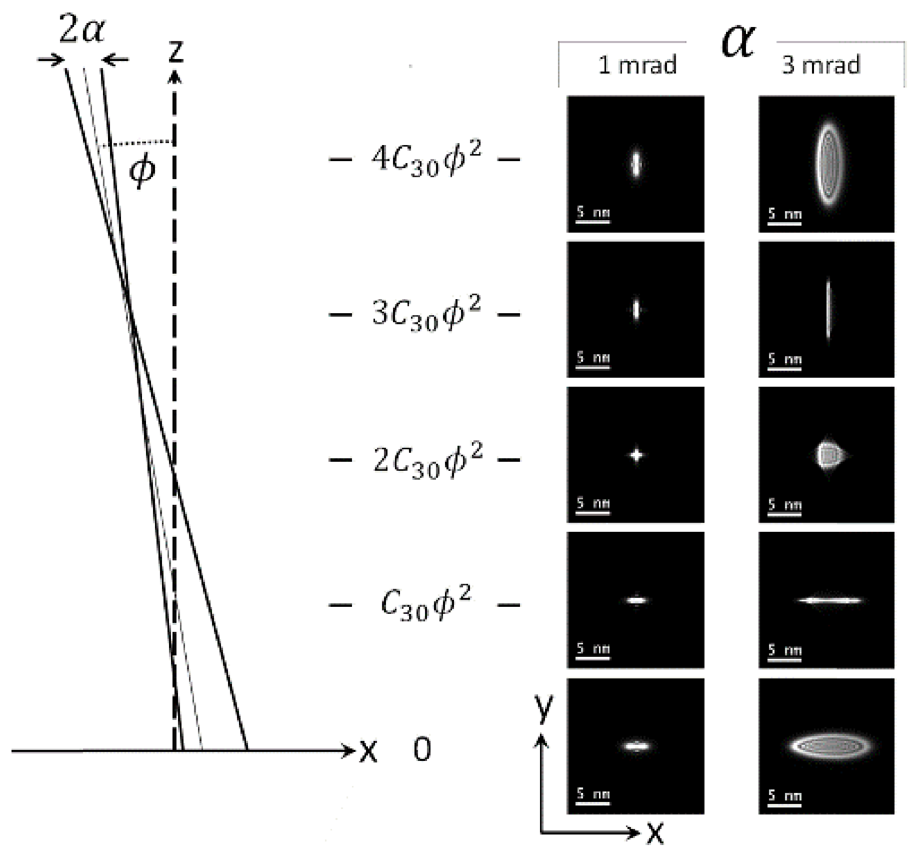

Demonstrating precession induced blur

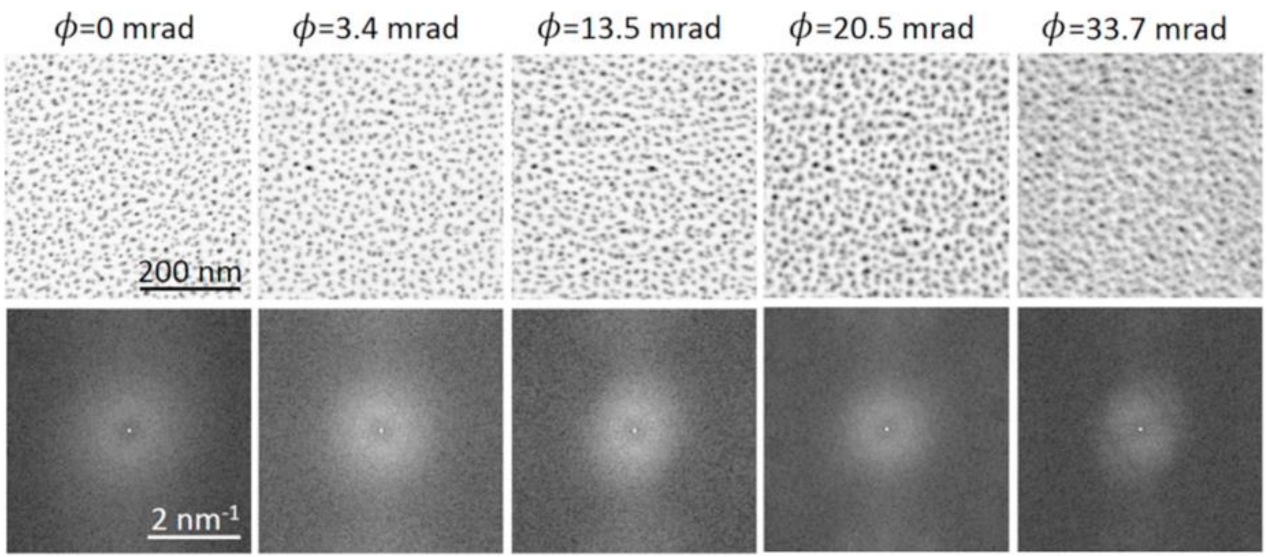

At higher precession angles Vincent-Midgley expression reasonable.

At lower angles we are limited by noise on the coils.

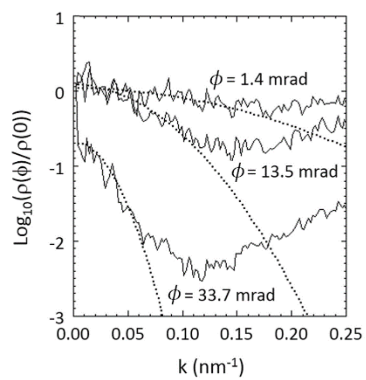

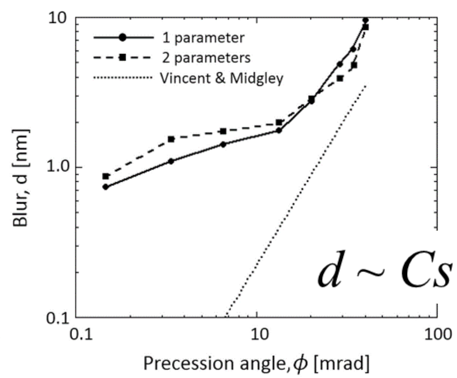

$$d \sim Cs\Phi^2\alpha$$

UNIVERSITY OF CAMBRIDGE

Part IV: Scanning Precession Electron Diffraction

Crystal Cartography

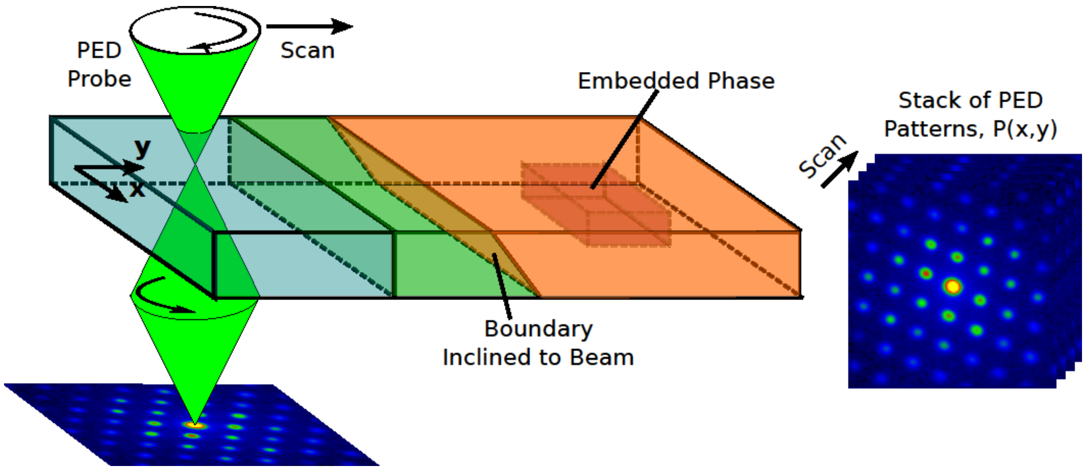

Typical precession: 100Hz
Dwell time = 20 ms
i.e. 50 patterns / sec
100x100 pixels in 2-3 min

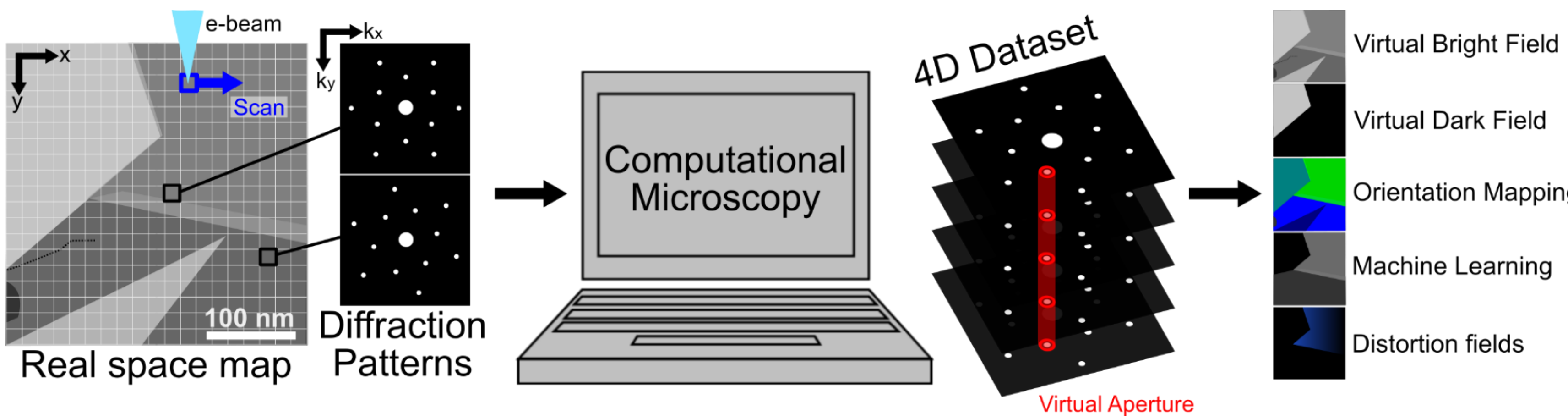

Strain mapping in (S)TEM

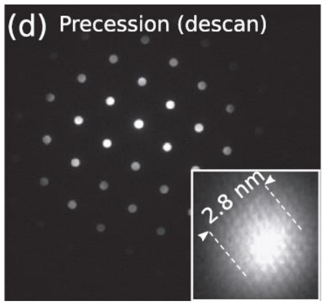

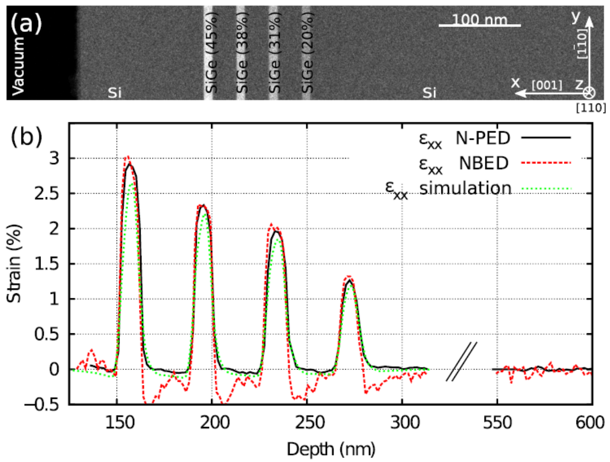

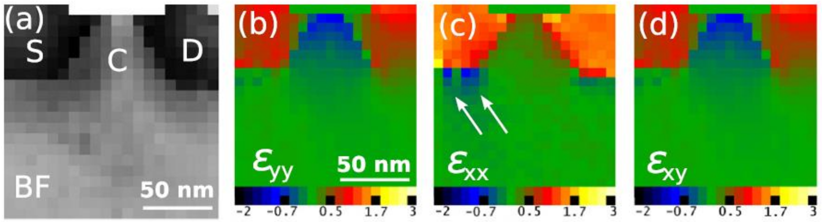

J.L. Rouviere et al
Appl. Phys. Lett.
103, 241913 (2013)

Strain (%) measured near the SiGe channel region of a transistor structure

Very small distortions in the PED patterns converted into local strain measurements.

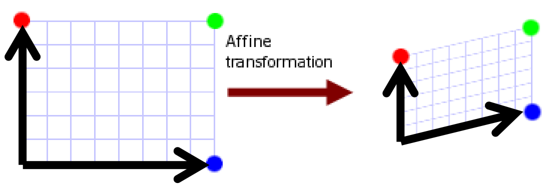

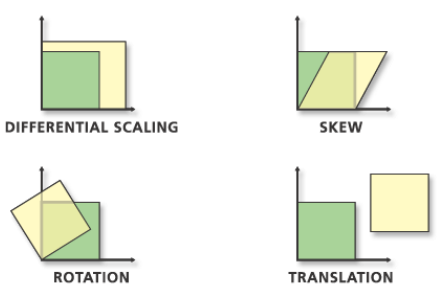

1. Lattice based
   - Find peaks.
   - Fit lattice to get basis vectors
   - Calculate affine transform between bases

2. Image processing
   - Calculate optimum affine transform directly between recorded patterns.

Strain Precision & Precession

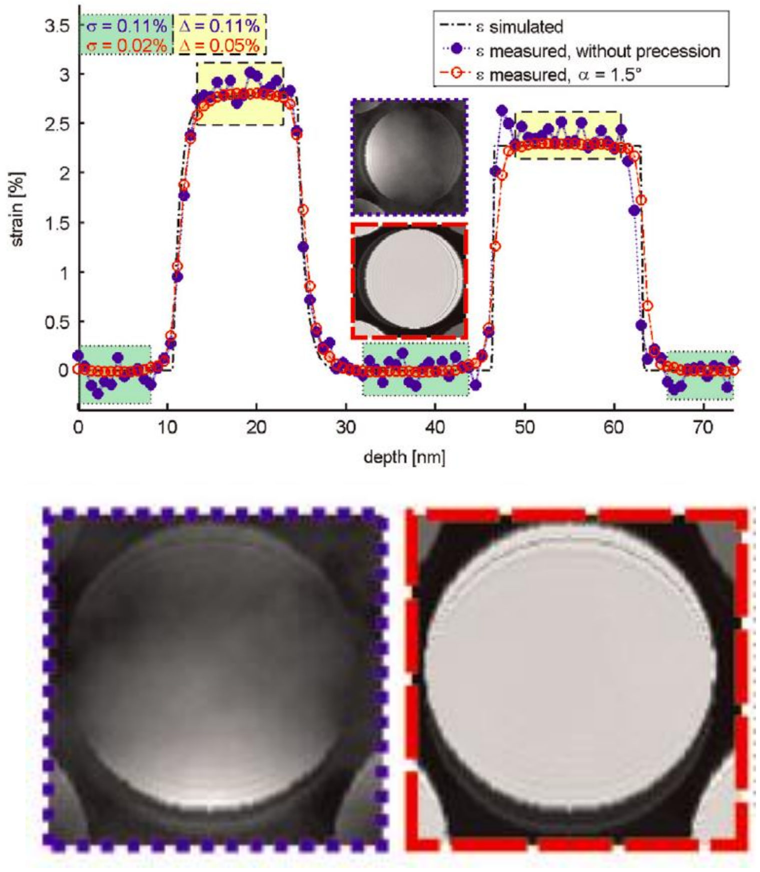

C. Mahr et al. Ultramicroscopy 158 (2015) 38 – 48

Precision with precession:

1. Integration through the Bragg condition means integration through bending & rel-rod effects.

2. Lattice plane distortions integrated through.

3. Homogeneously filled CBED disks are easier to track in computational analysis.

Typically claim ~2e-4

Based on rms error in unstrained region.

Phase & Orientation Mapping: A wider view

EBSD/TKD

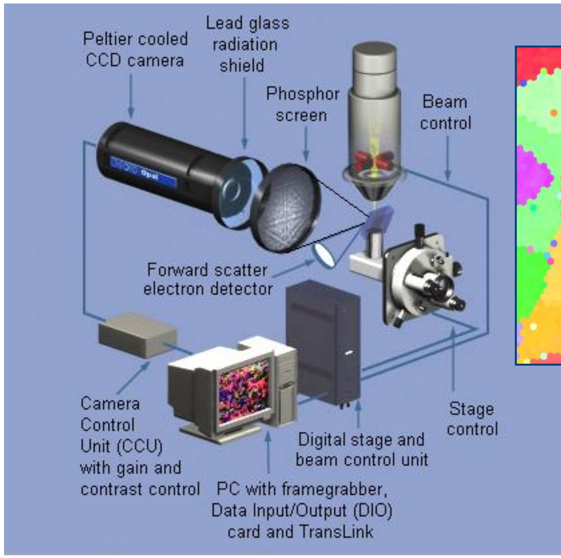

SPED

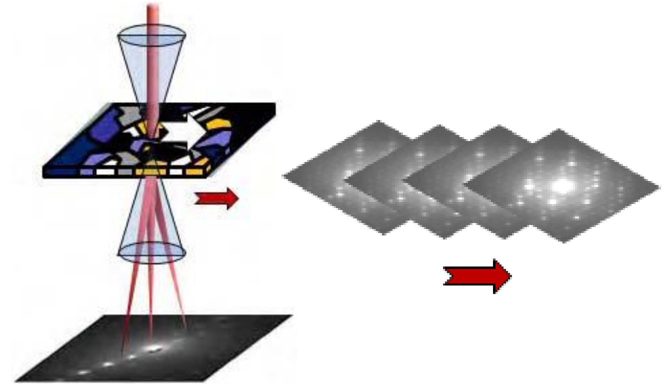

X-ray Laue

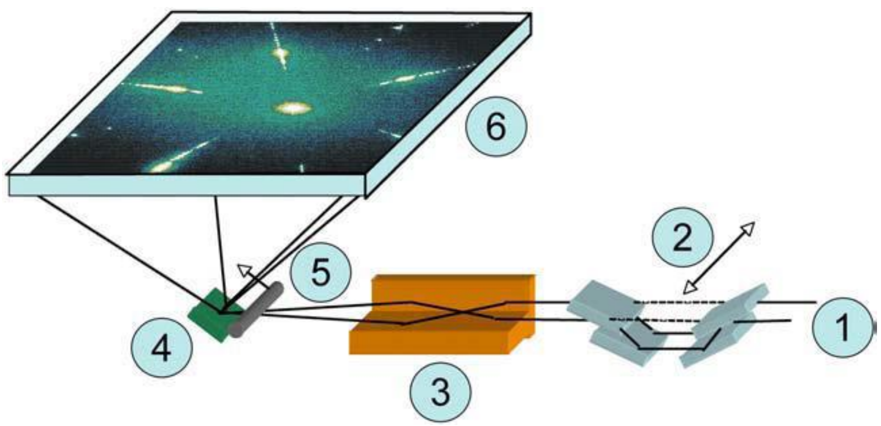

Tomography

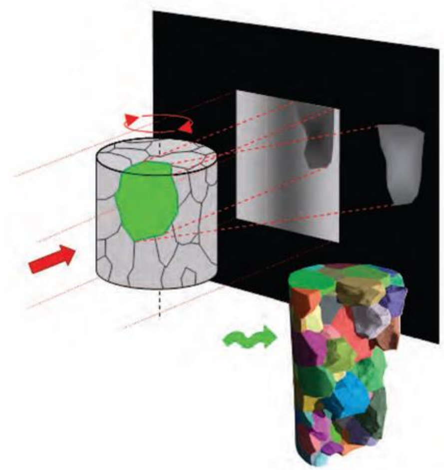

Orientation Mapping via Template Matching

Improved reliability of template matching with PED

D. Viladot et al, *J. Microscopy*, 252, 2013, 23–34

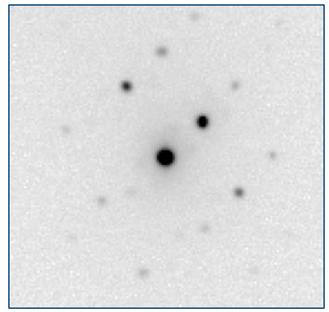

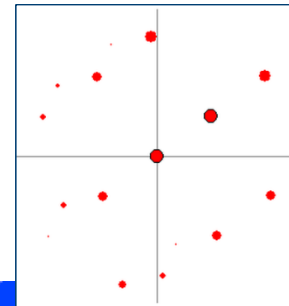

Colour scheme indicates orientation (z-vector)

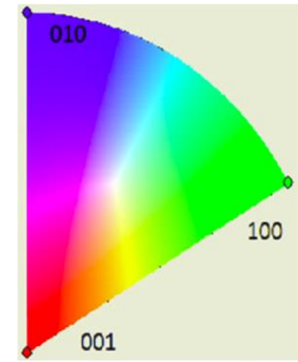

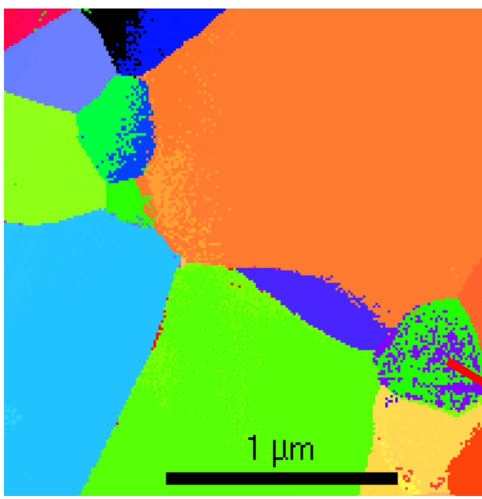

Al_2O_3 sample (trigonal, R3c; a = 4.78 A, c = 12.99 A)

Unprecessed

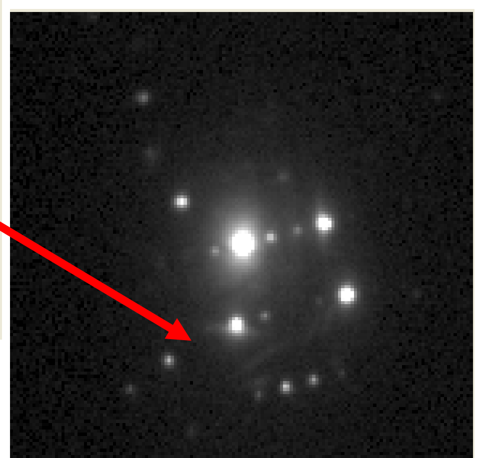

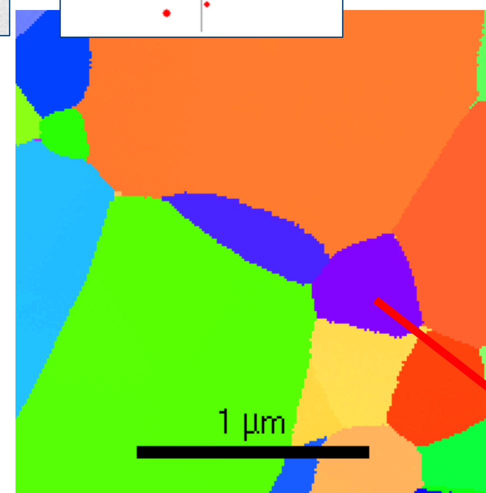

0.5° precession

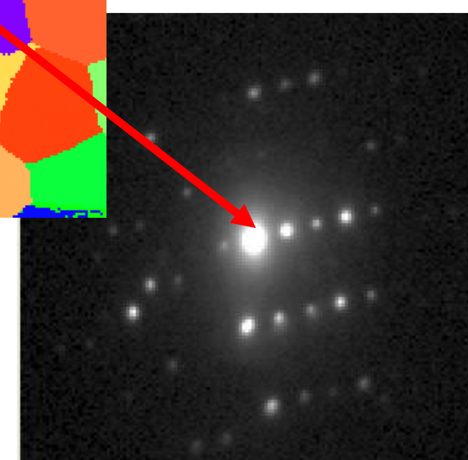

Orientations & Misorientations

Orientations

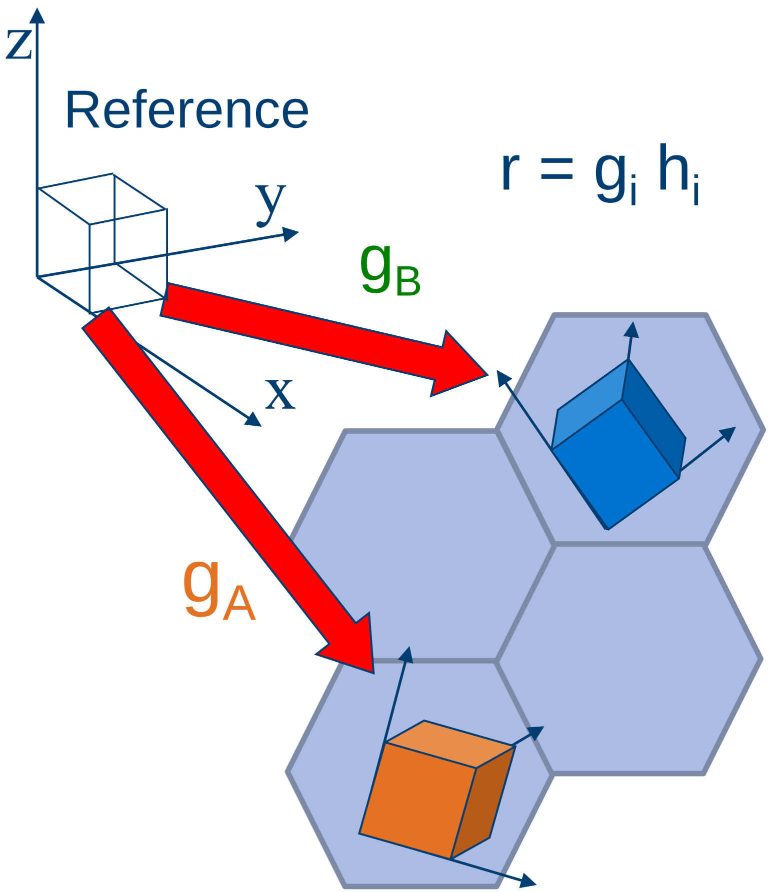

Misorientations

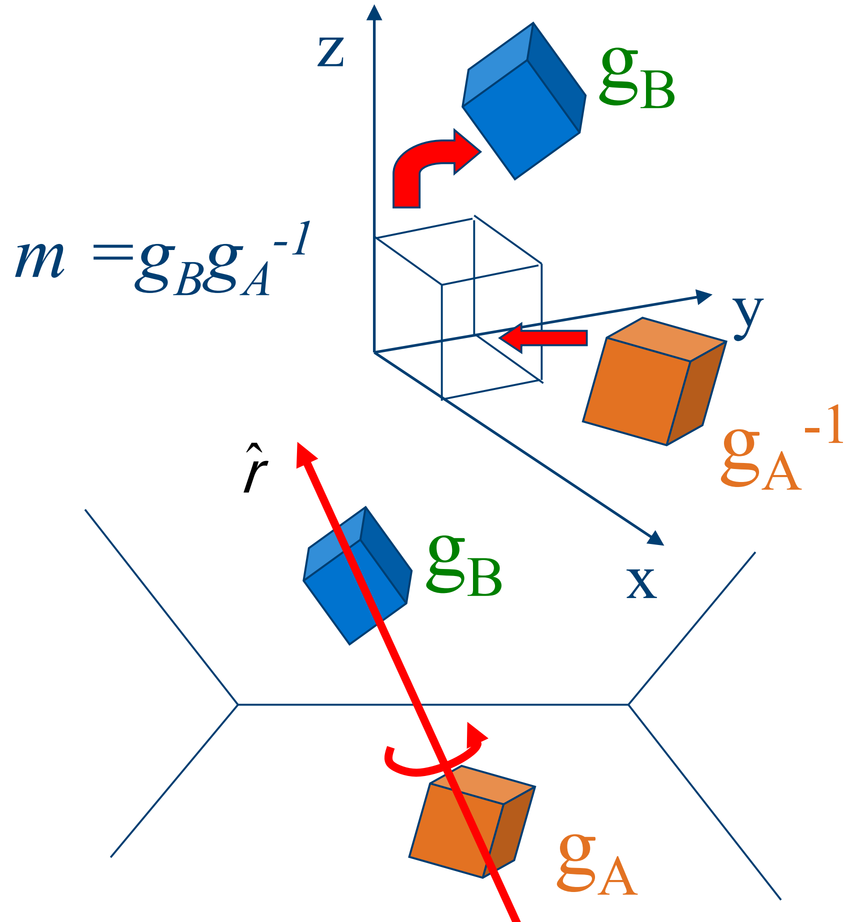

Standard ways to represent orientations

Pole Figure

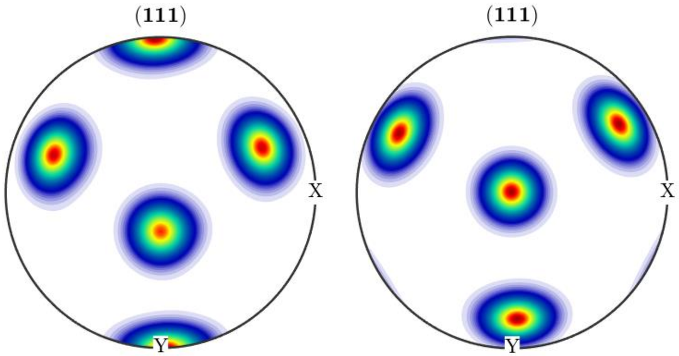

Crystal plane normals plotted in specimen coordinate system.

Inverse Pole Figure

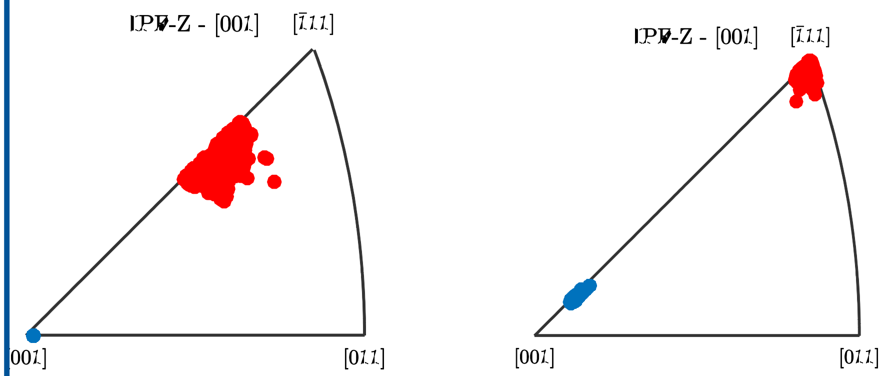

Specimen directions in crystal coordinate system (with symmetry applied).

Orientation Images

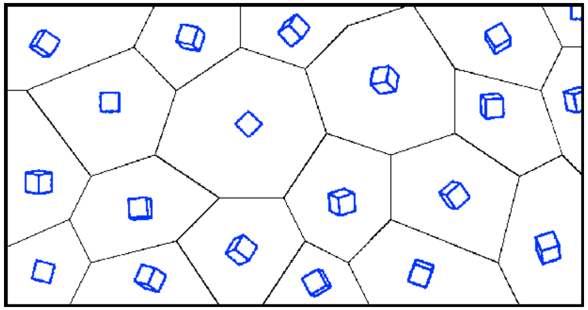

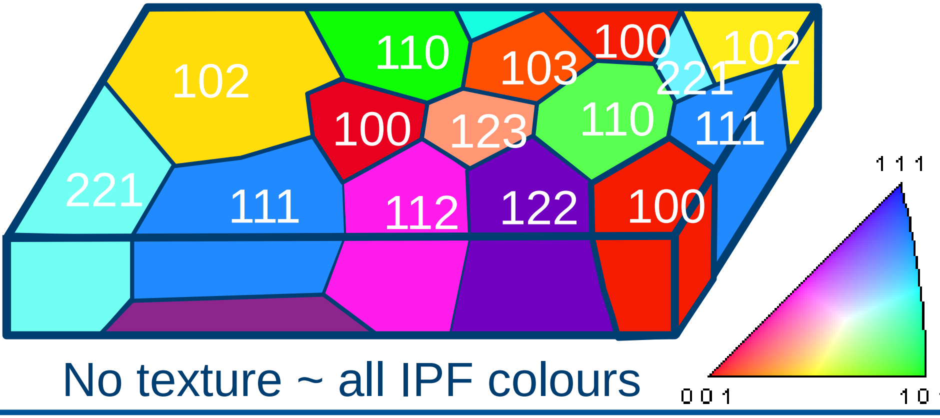

No texture ~ all IPF colours

Neo-Eulerian representations of orientations

A rotation may be described by a rotation axis ***r*** and angle *α*:

$\mathcal{R}(\mathbf{r}, \alpha)$

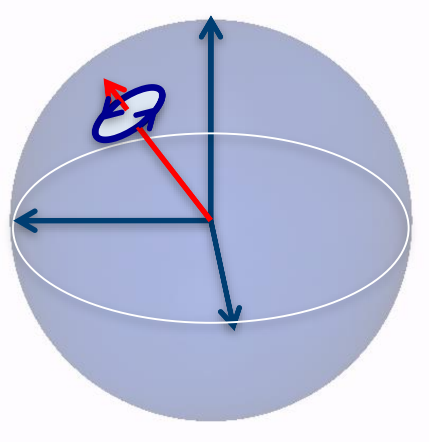

Numerous Parameterisations:

- $p = r\,a$
- $p = r \tan(a/2)$
- $p = r \sin(a/2)$
- $p = r\,\{3/4(a - \sin a)\}^{1/3}$
- $p = r\,2 \tan(a/4)$

Symmetry reduces orientation space to a *fundamental zone*

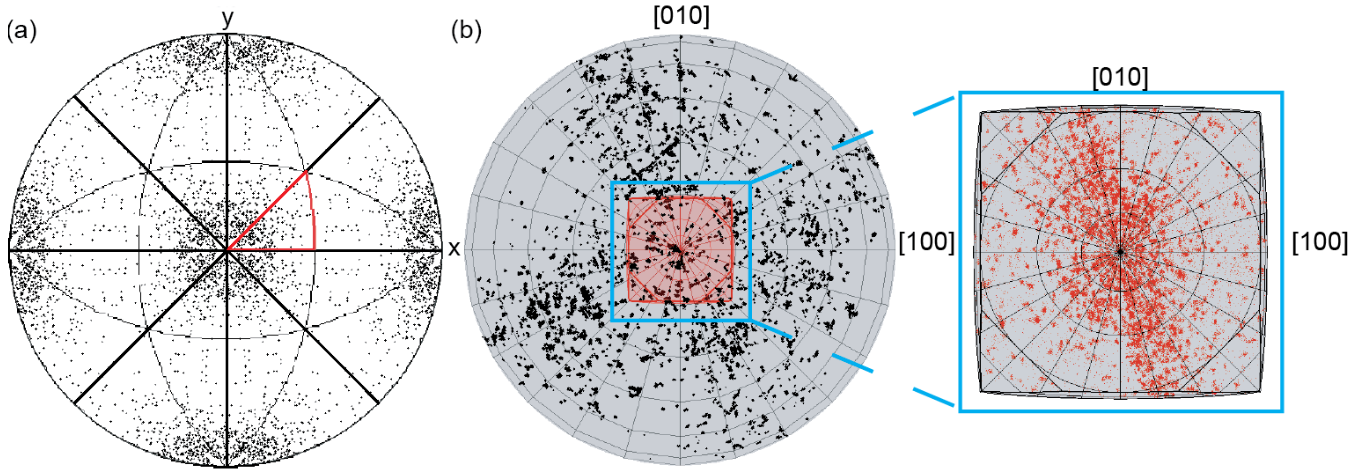

Fundamental zones for orientations

All fundamental zones for orientations

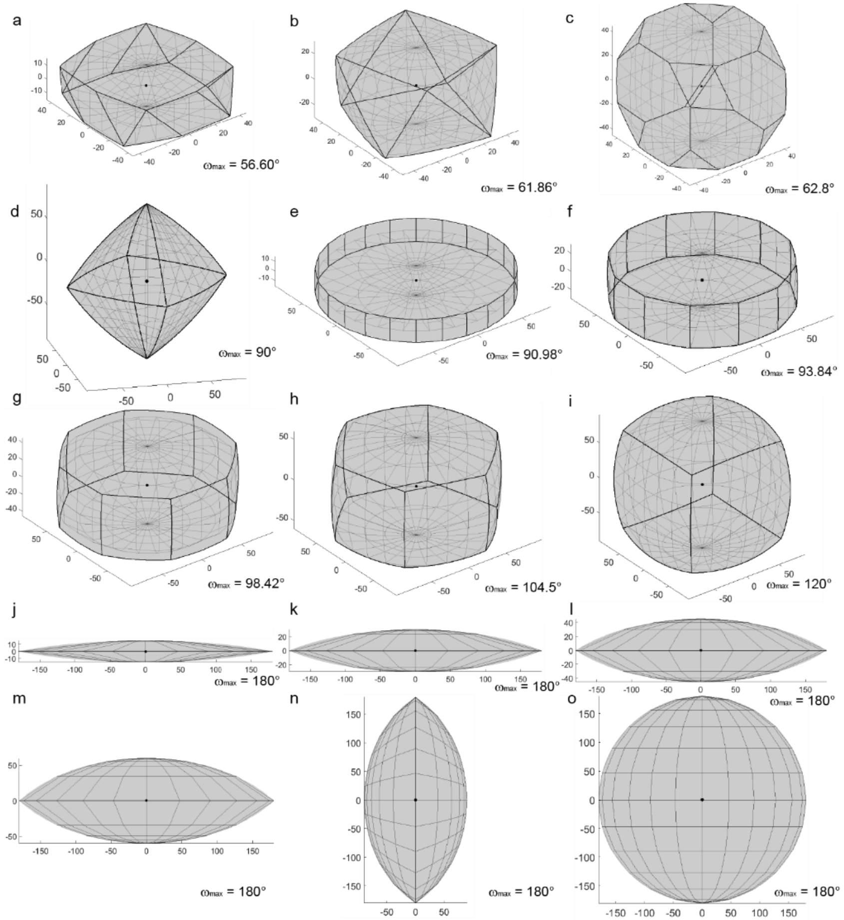

Symmetry reflected in geometry

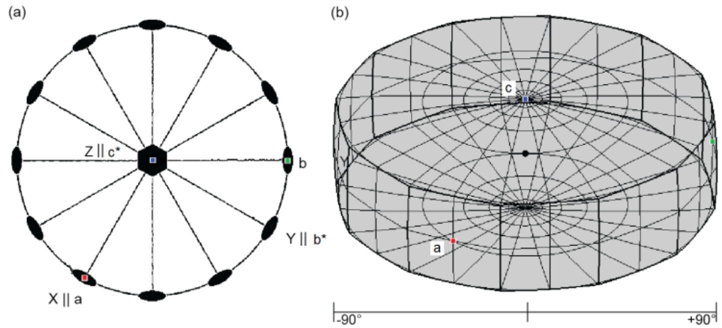

Boundary points have equivalents

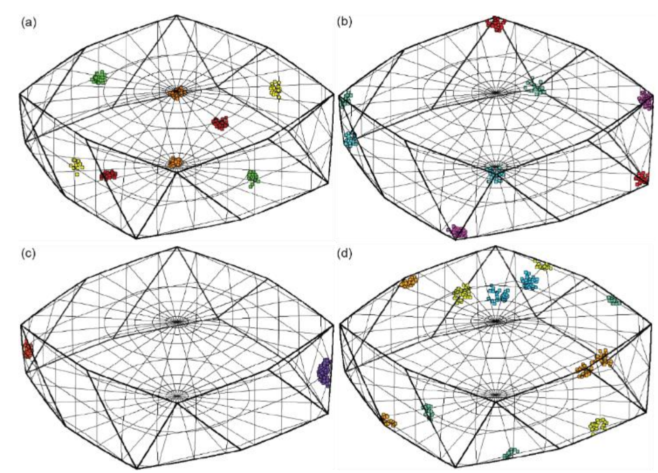

Fundamental zones for misorientations

Depends on the symmetry of both crystals

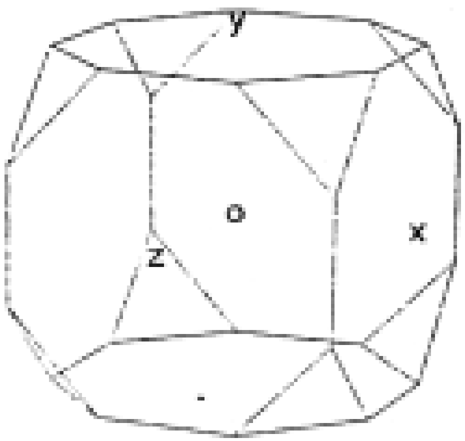

Cubic crystal symmetry,
no sample symmetry

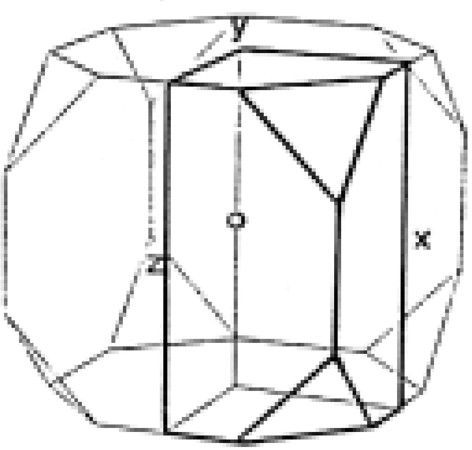

Cubic-orthorhombic

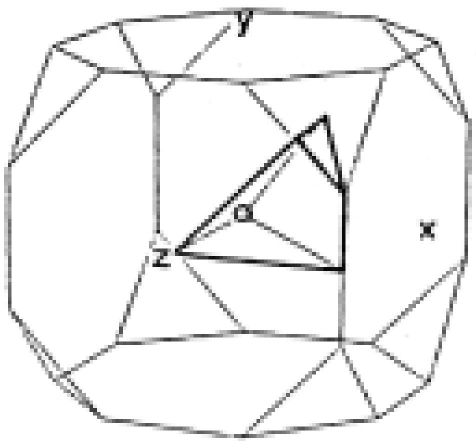

Cubic-cubic symmetry

All fundamental zones for misorientations are sections of the fundamental zone for orientations of the reference crystal symmetry.

Case Study: Inter-phase relationships in ATI 718Plus

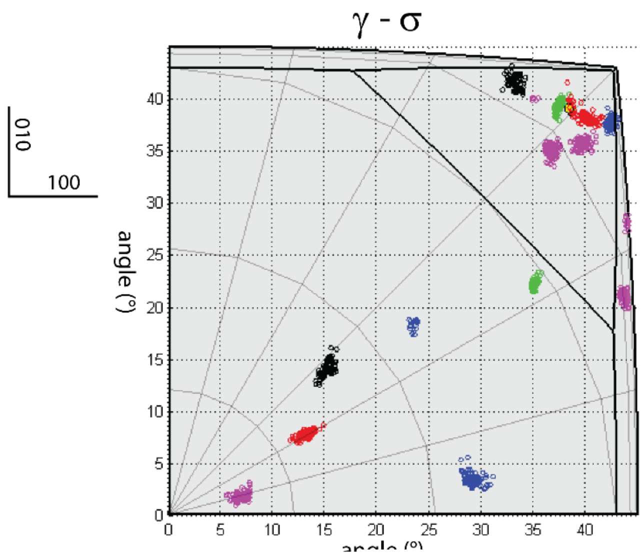

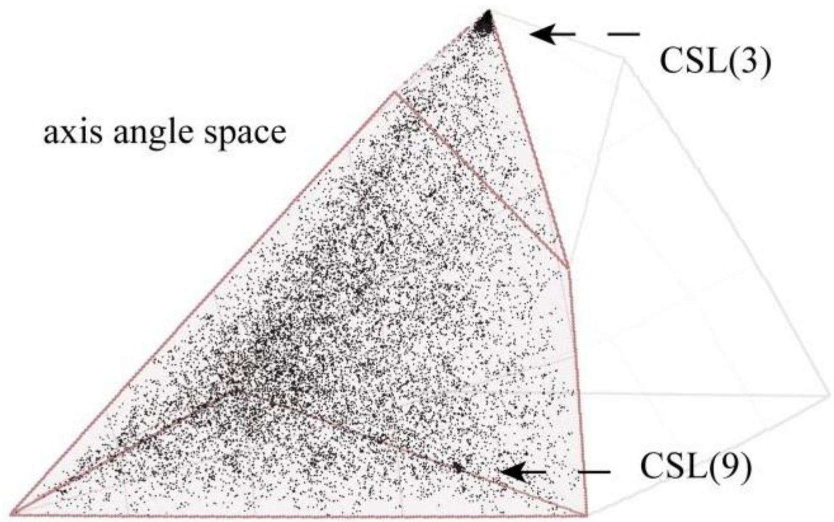

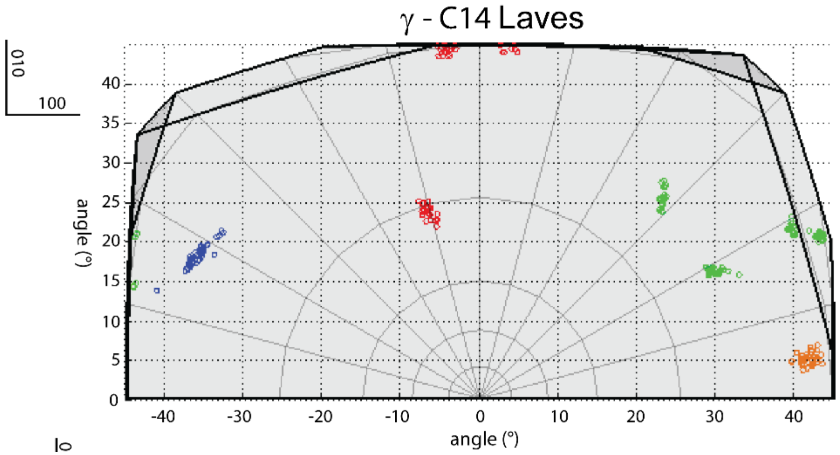

Projection problem: need to separate mixed signals

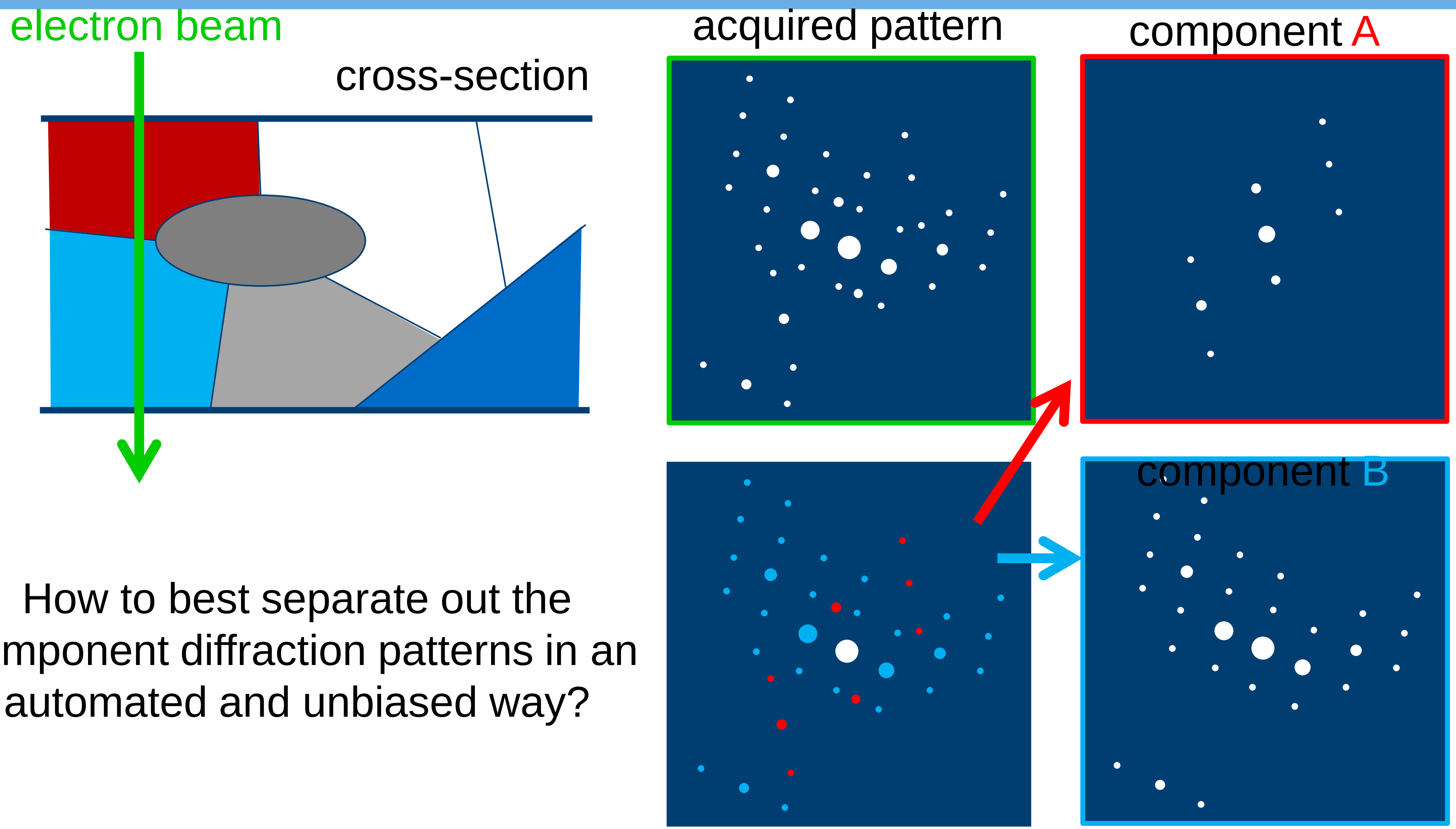

How to best separate out the component diffraction patterns in an automated and unbiased way?

Can we separate mixed signals using all the data?

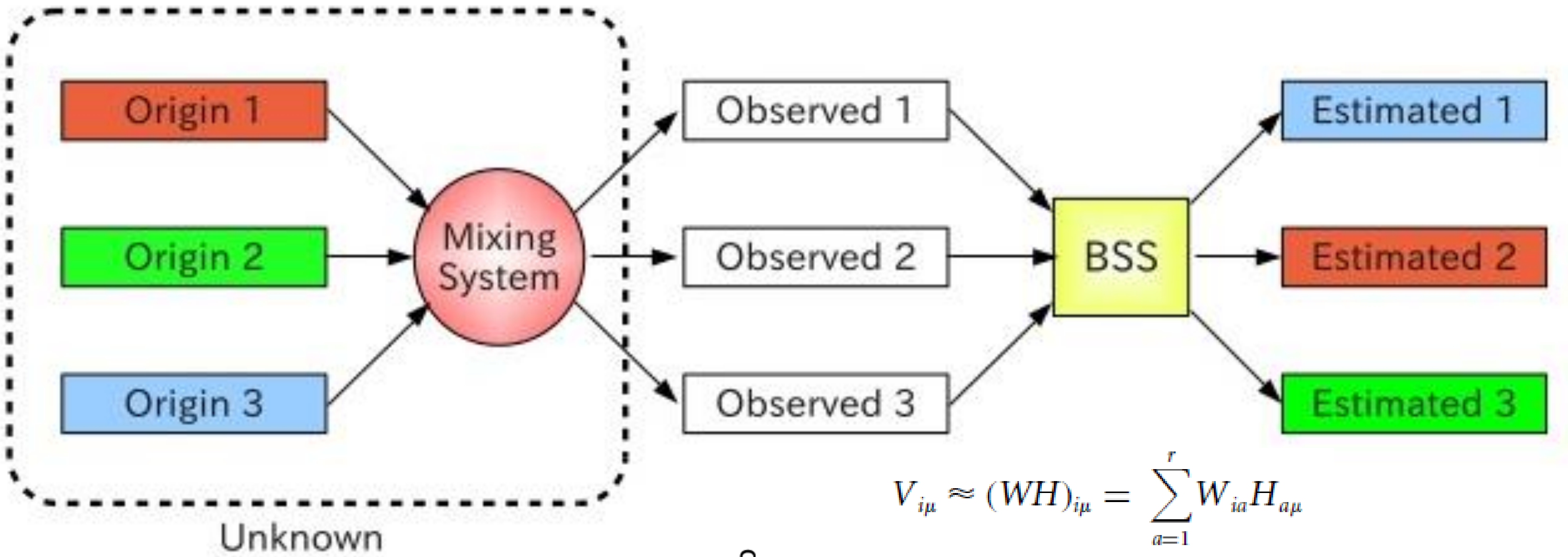

$$V_{i\mu} \approx (WH)_{i\mu} = \sum_{a=1}^{r} W_{ia} H_{a\mu}$$

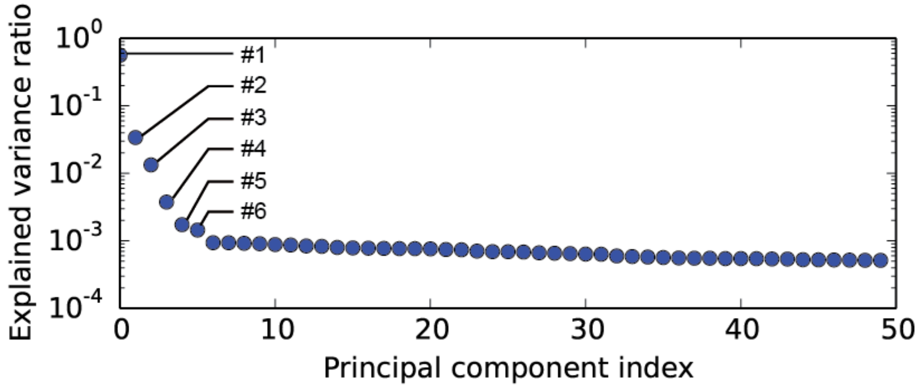

Use PCA scree plot to estimate the number of components

Blind source separation in spectrum imaging

Basis spectra statistically 'independent'

$$S_m = \sum_{n=1}^{N} W_n H_{nm}$$

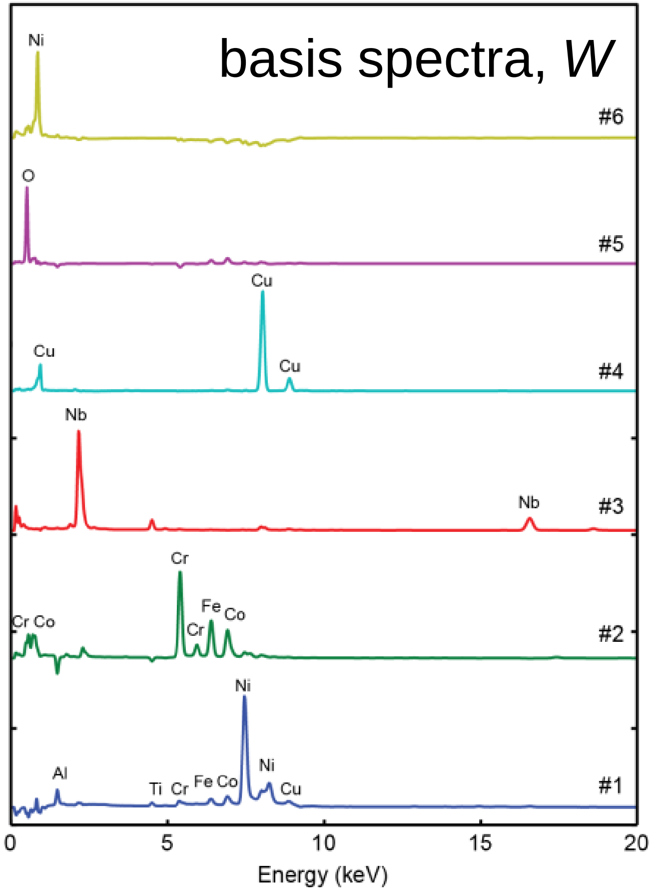

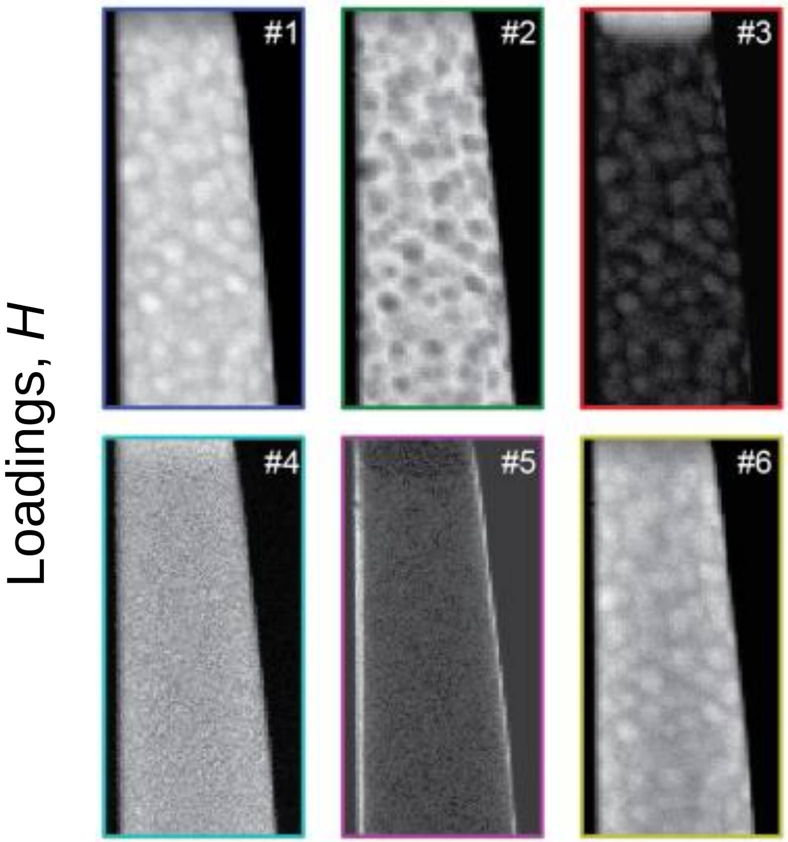

Machine Learning SPED

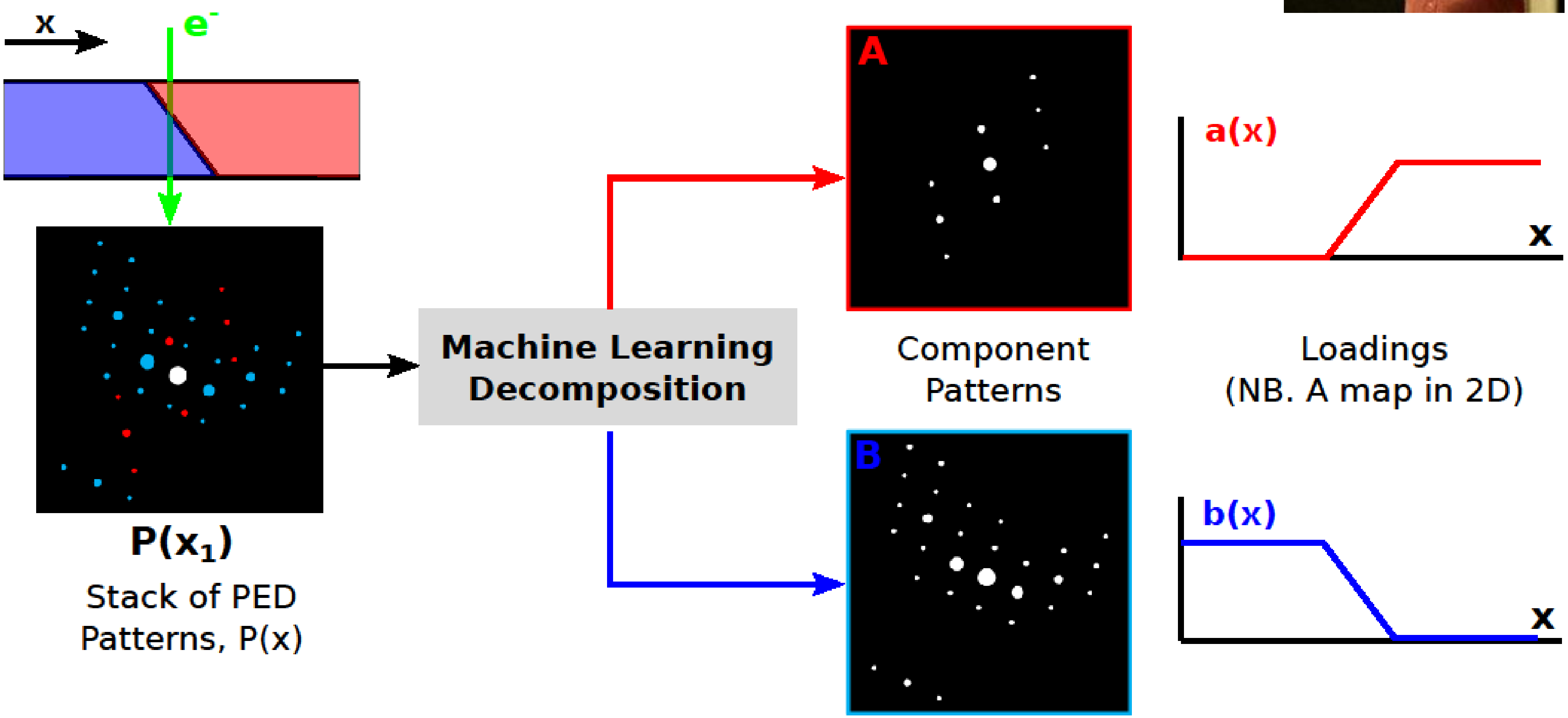

$$P(x_1) \sim a(x_1)A + b(x_1)B$$

Which Method of Unsupervised Learning?

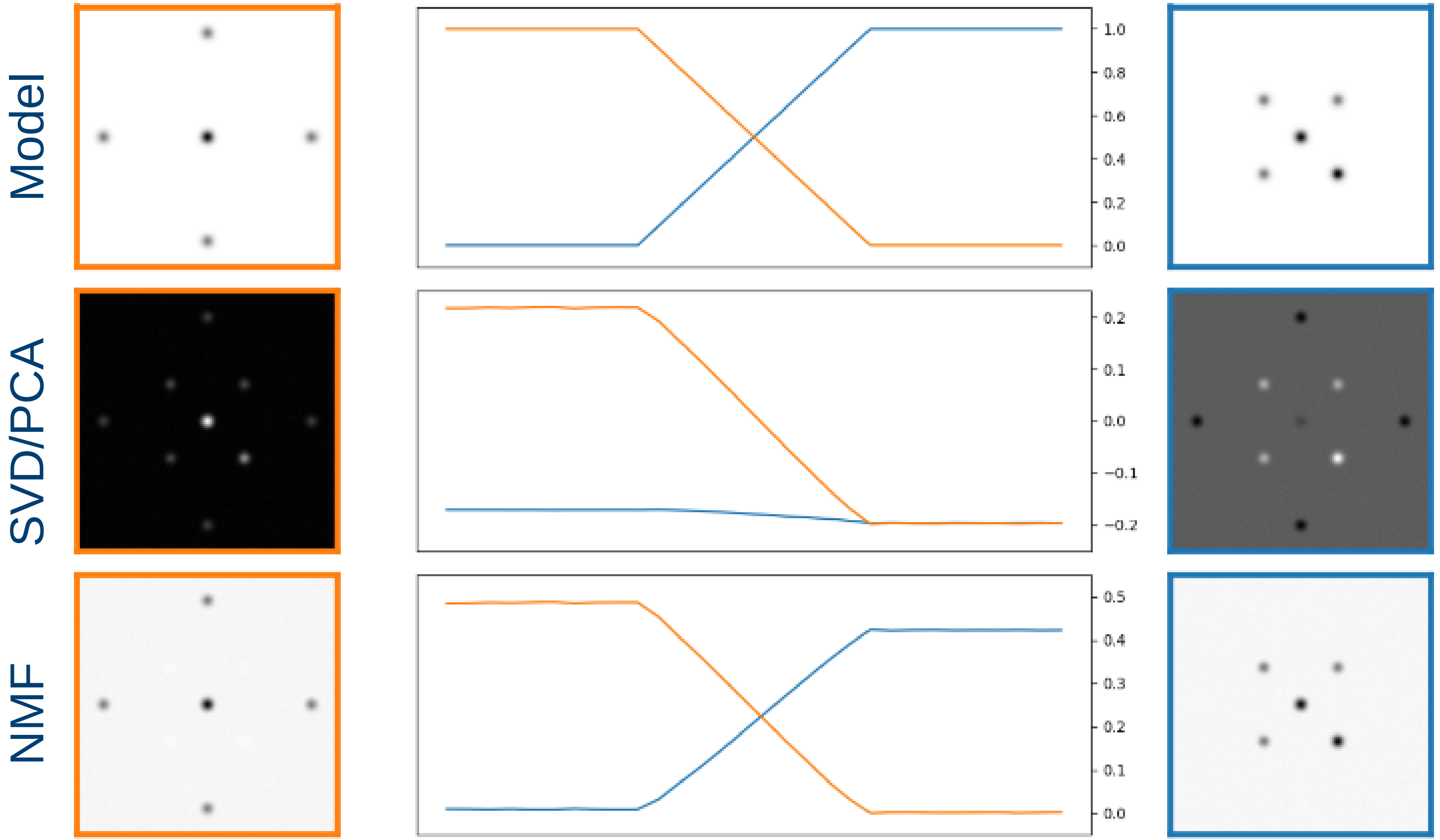

PCA/SVD does not obtain physical patterns. NMF giving physical constraints does!

NMF, theoretical data, and precession

Multi-slice simulation of GaAs rotation twin boundary inclined to the beam direction. 200 precession steps, thickness ~ 150nm.

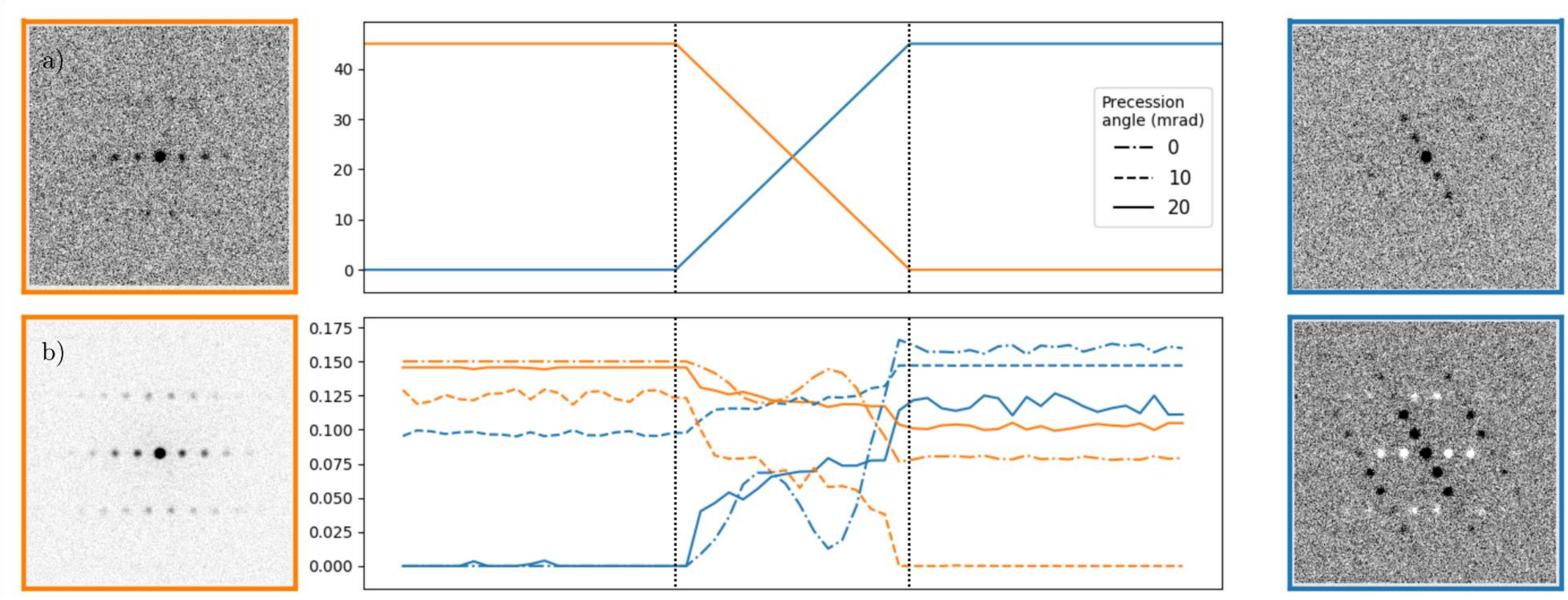

NMF loading becomes more monotonic with increasing precession angle.

NMF, experimental data and precession

Precession integrates bending

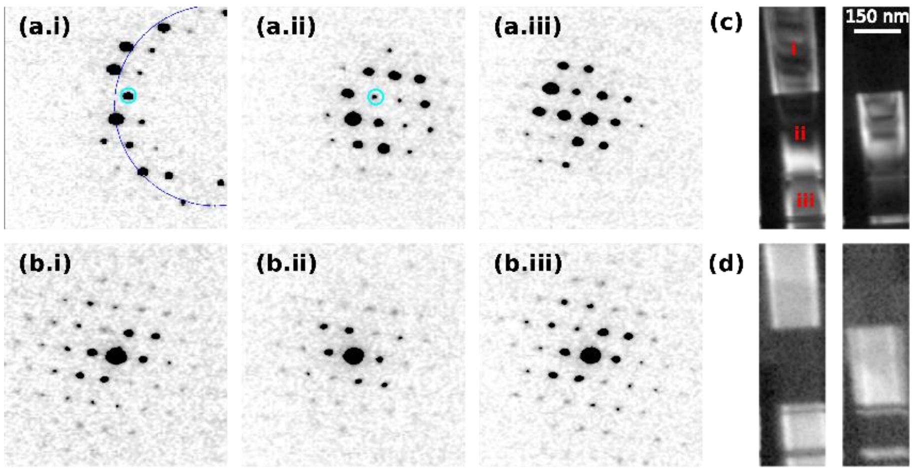

With precession can separate signal from noise

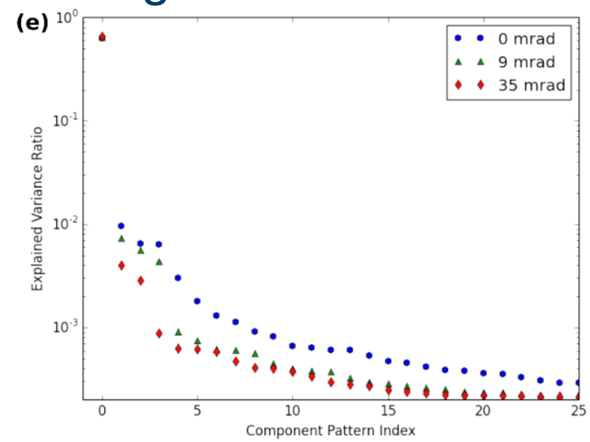

With precession overlap is revealed with reasonable accuracy

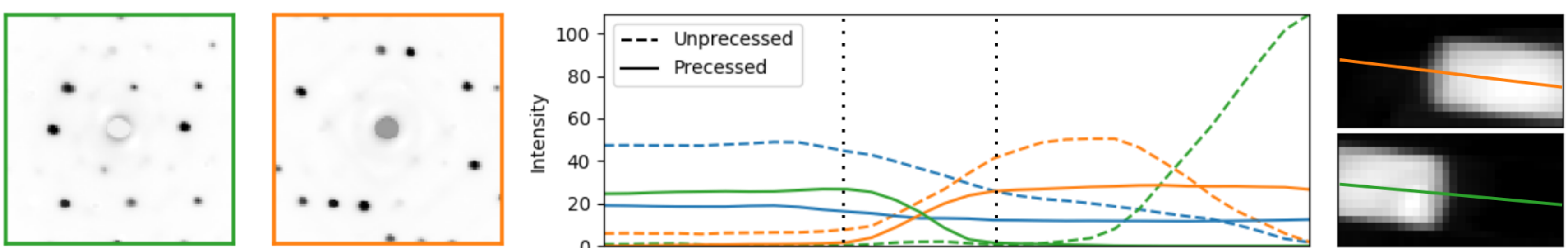

Summary

1. Strain mapping
    - Precession improves precision
2. Orientation mapping
    - Precession aids matching
    - Orientation analysis can be taken much further than colour maps
3. Machine Learning
    - Precession necessary to separate physically interesting signal
    - Results reduce the diffraction data to essential components guiding further, more detailed, analysis.

UNIVERSITY OF CAMBRIDGE

Part V: Scanning Precession Electron Tomography

What about crystallographic mapping in 3D?

(A) X-RAY. Diffraction Contrast X-ray Tomography – using images

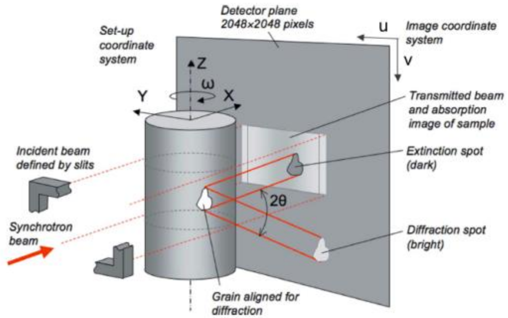

Figure 1
An overview of the acquisition geometry, showing the cropped synchrotron beam, the sample, and both direct and diffracted images on the detector.

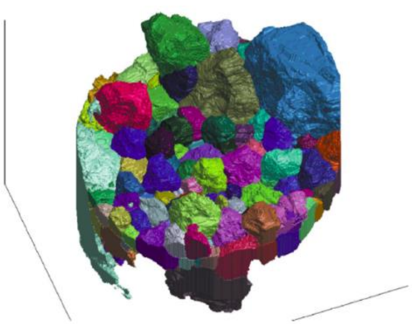

Al alloy
FOV = 500 um
Voxel size ~1um

G. Johnson et al, *J. Appl. Cryst*. (2008) 41, 310–318

(B) TEM. 3D grain orientation – tilt series of HCDF images

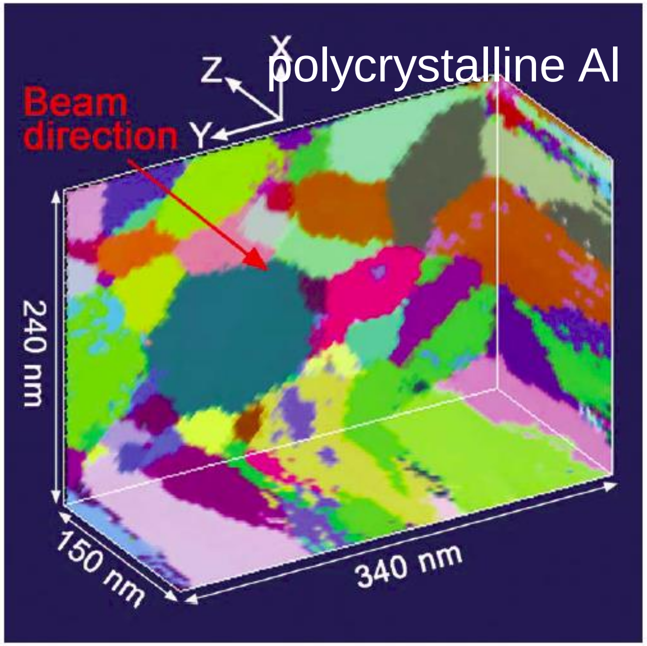

More than 100,000 dark field images recorded +/-30° @ 1°. At each sample tilt, the beam rotation angle varied 0 - 360° in steps of 2°.

H.H. Liu et al *Science* 332 (2011) 833

Projection problem: need to separate mixed signals

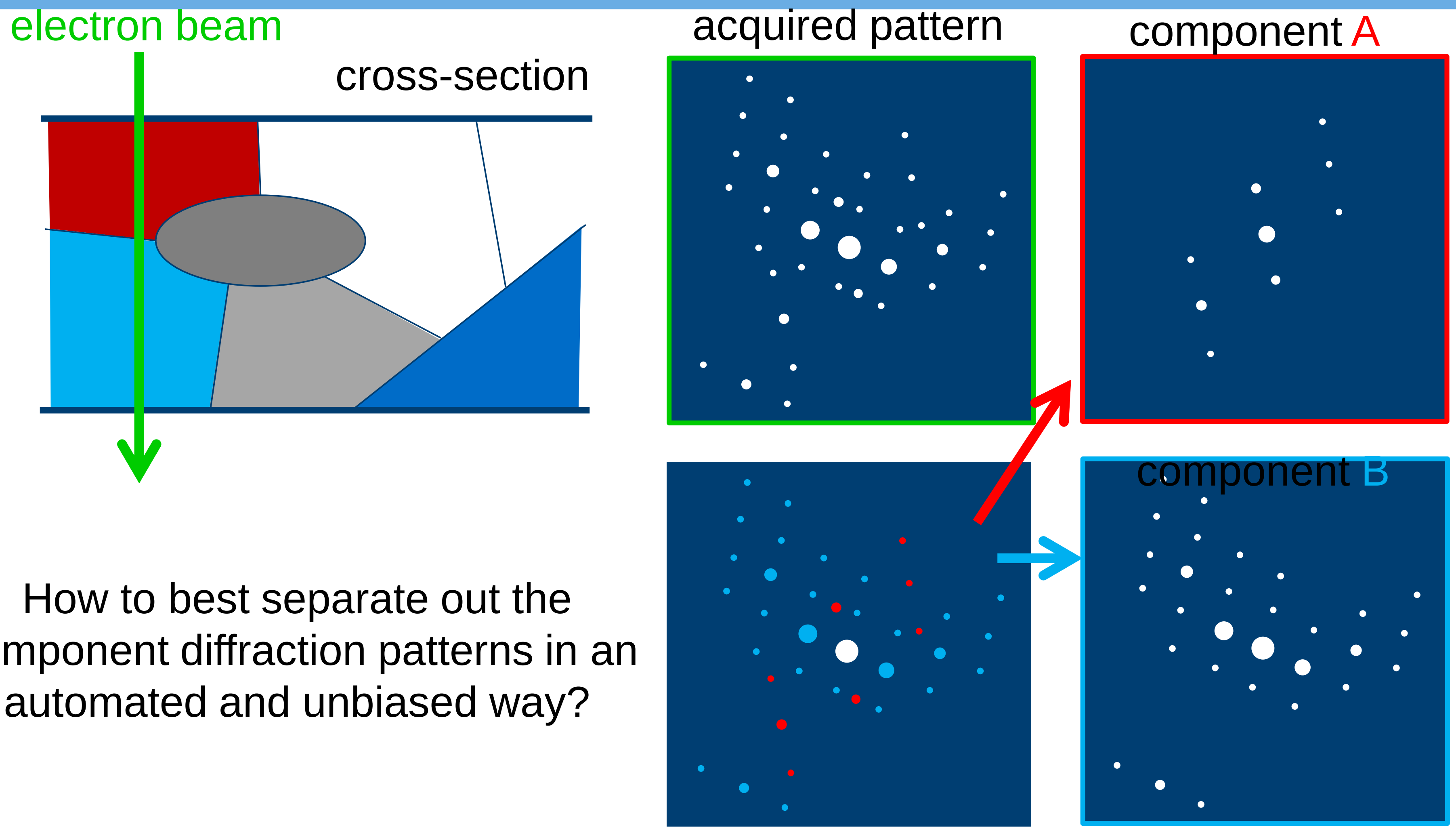

How to best separate out the component diffraction patterns in an automated and unbiased way?

SPED Tomography of 718+

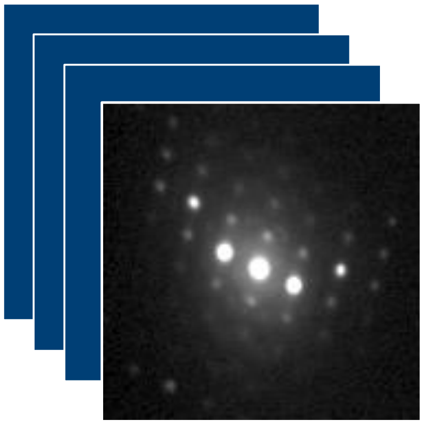

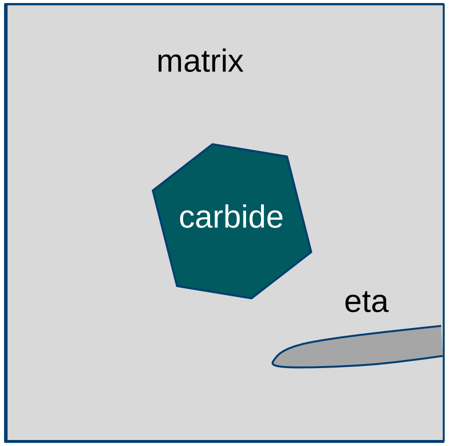

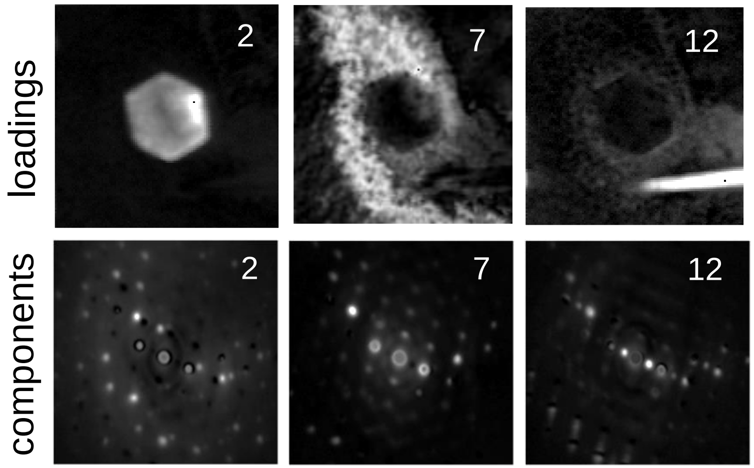

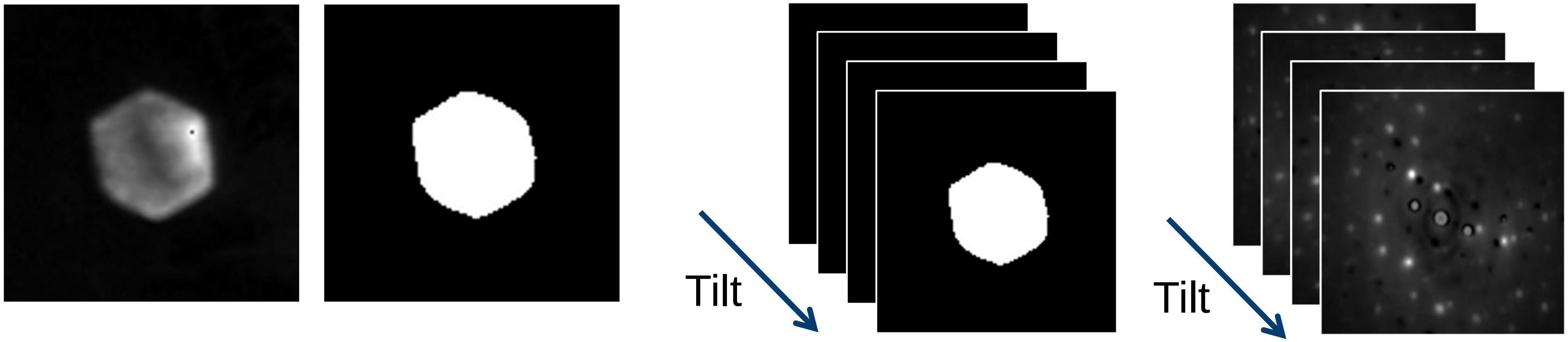

Real & Reciprocal Space in 3D

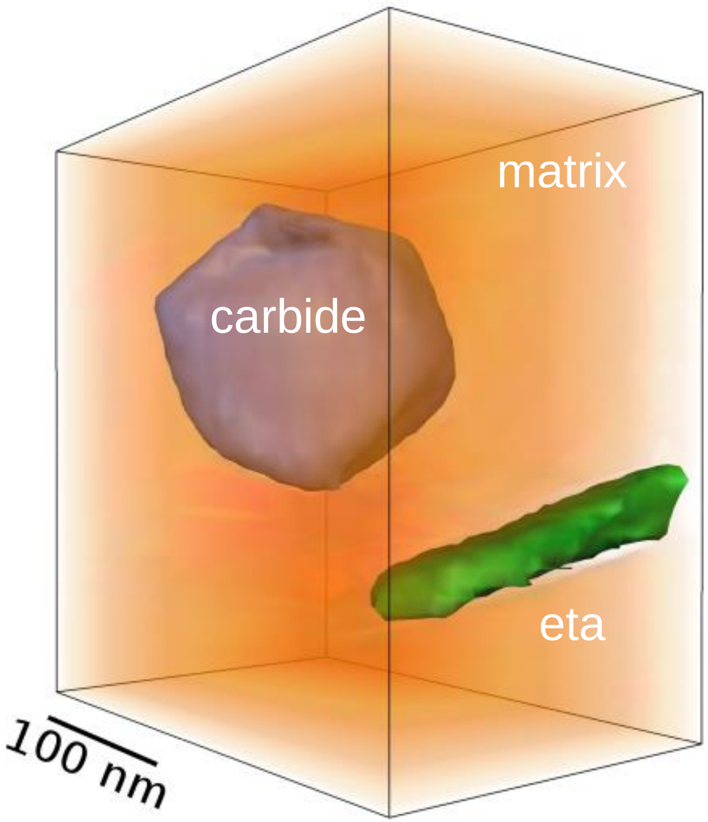

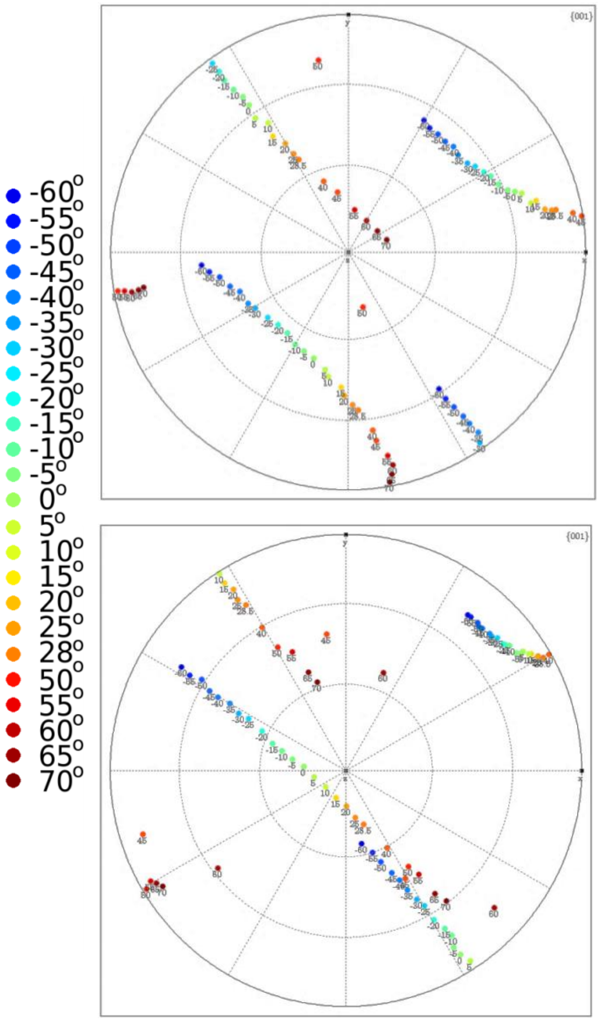

matrix component

carbide component

Orientation Relationship in 3D

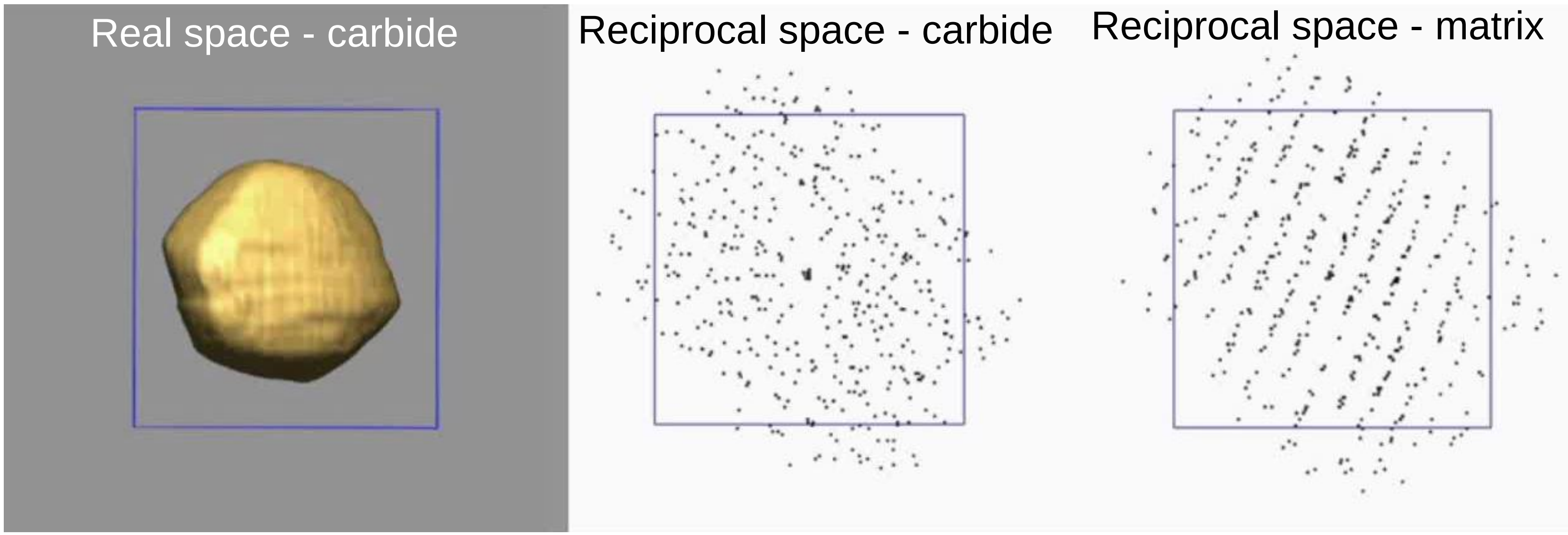

$[111]_c$ $[5\bar{3}\bar{1}]_m$

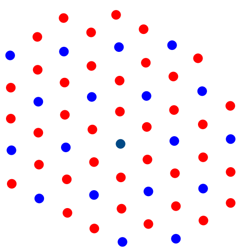

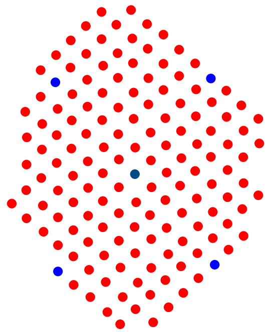

$[111]_c$

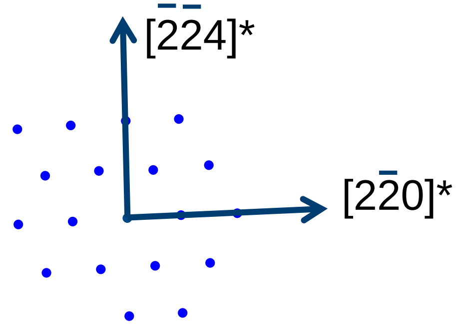

$[5\bar{3}\bar{1}]_m$

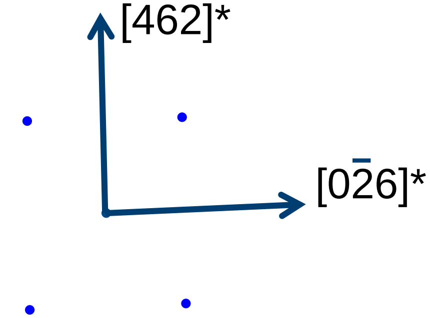

Orientation Relationship in 3D

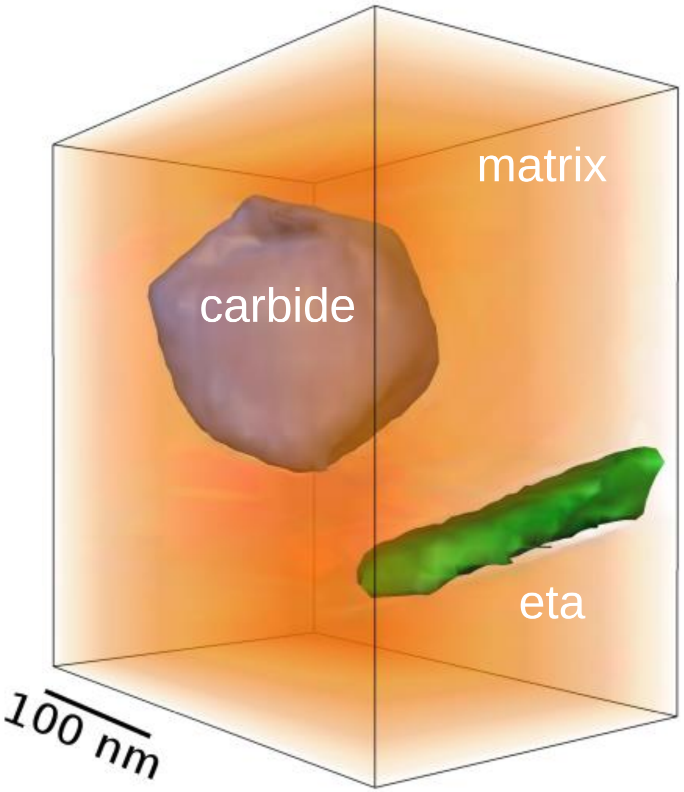

$\{111\}_{carbide}$ // $\{531\}_{matrix}$

$[220]^*$ // $[026]^*$

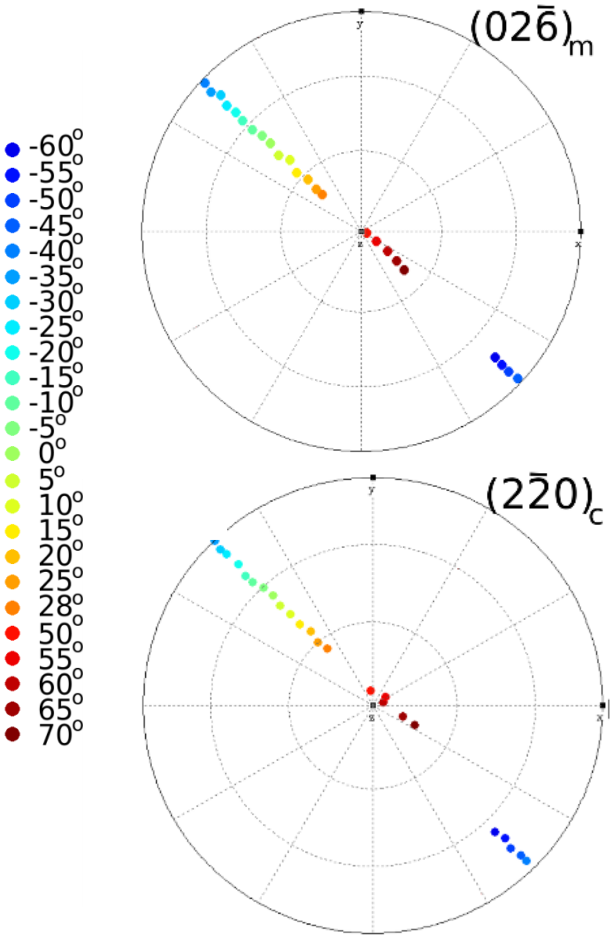

matrix component

carbide component

Case Study: GaAs Nanowires

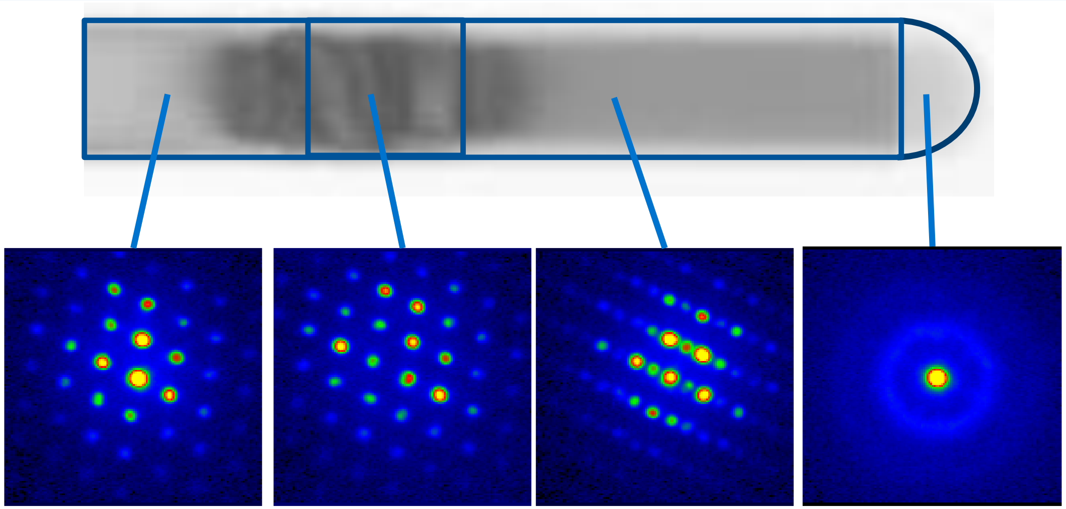

27 mrad

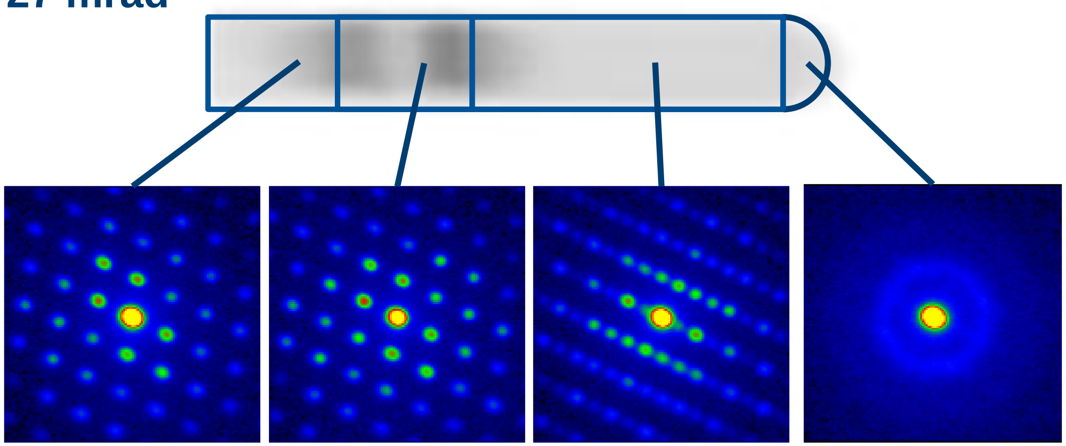

$(111)_{ZB} \,||\, (0002)_{WZ}$

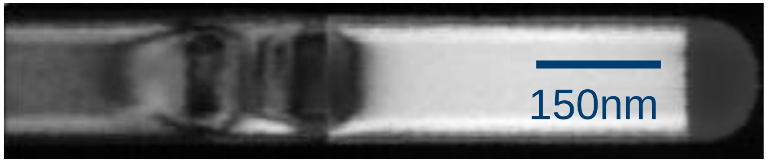

$(224)_{ZB}$

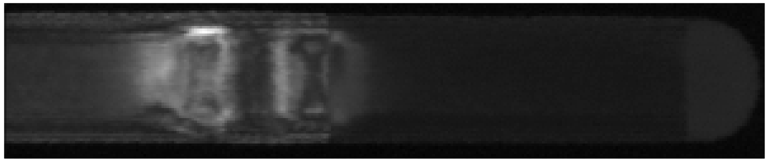

Diffuse

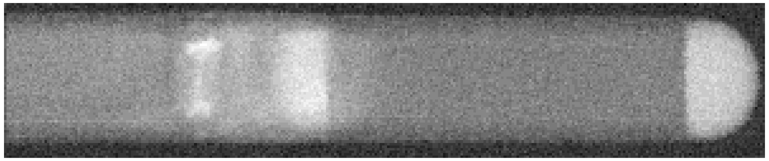

Towards Strain Tomography

1. Map strain at every pixel

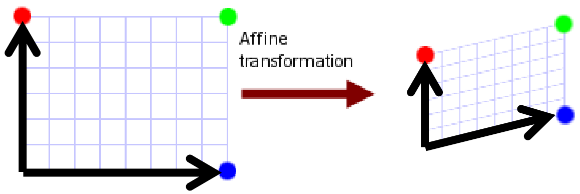

$$x' = D\,x + t$$
$$D = R\,F$$
$$\varepsilon = F - I$$

2. Mapped strain is average along beam path

$$\langle \varepsilon \rangle = \frac{\int_{-\infty}^{\infty} \varepsilon(x)\, ds}{\int_{-\infty}^{\infty} ds}$$

3. Projected component of strain

$$J\varepsilon(x) = \int_{-\infty}^{\infty} \varepsilon\,(x)\, ds$$

4. Reconstruct as scalar tomography

Tilt Series // <111>

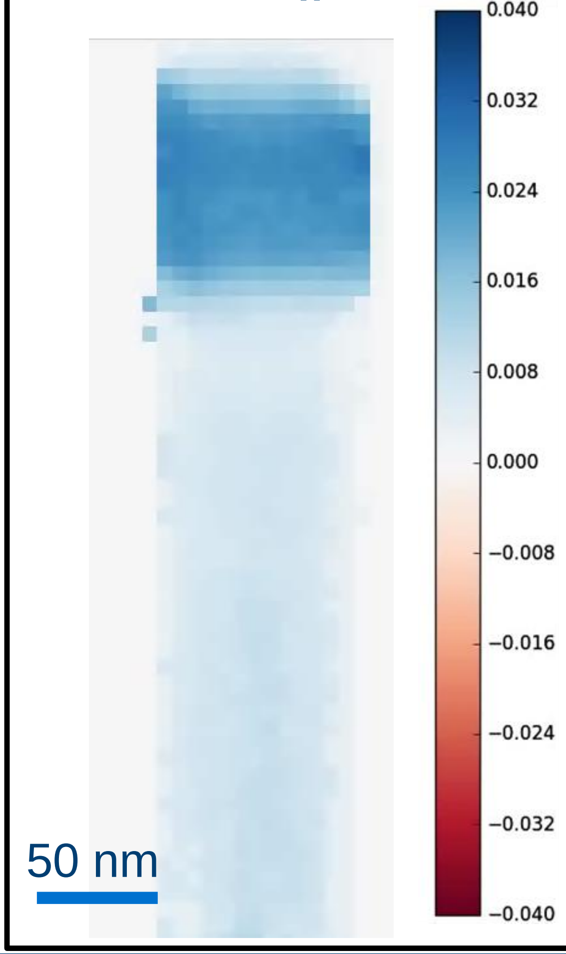

UNIVERSITY OF CAMBRIDGE

Towards Strain Tomography - $\varepsilon_{rod}(x)$ reconstruction

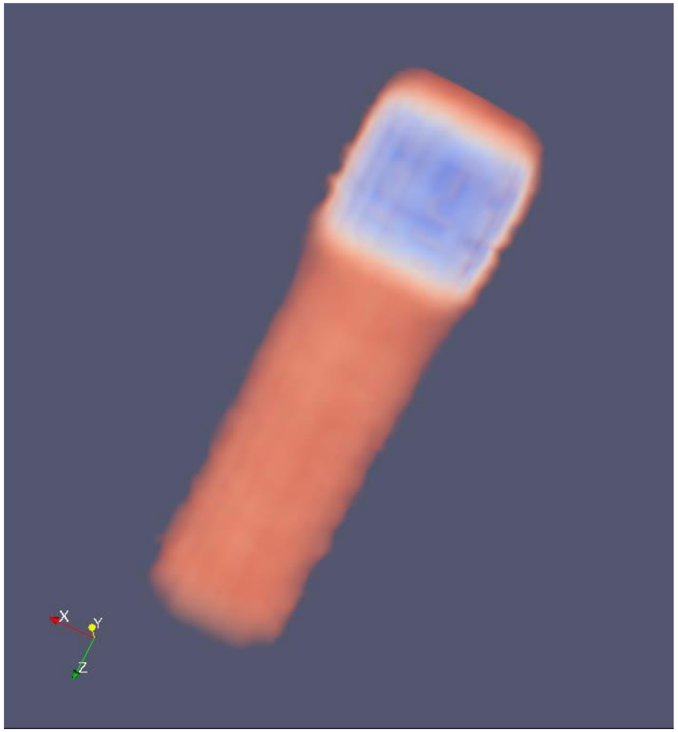

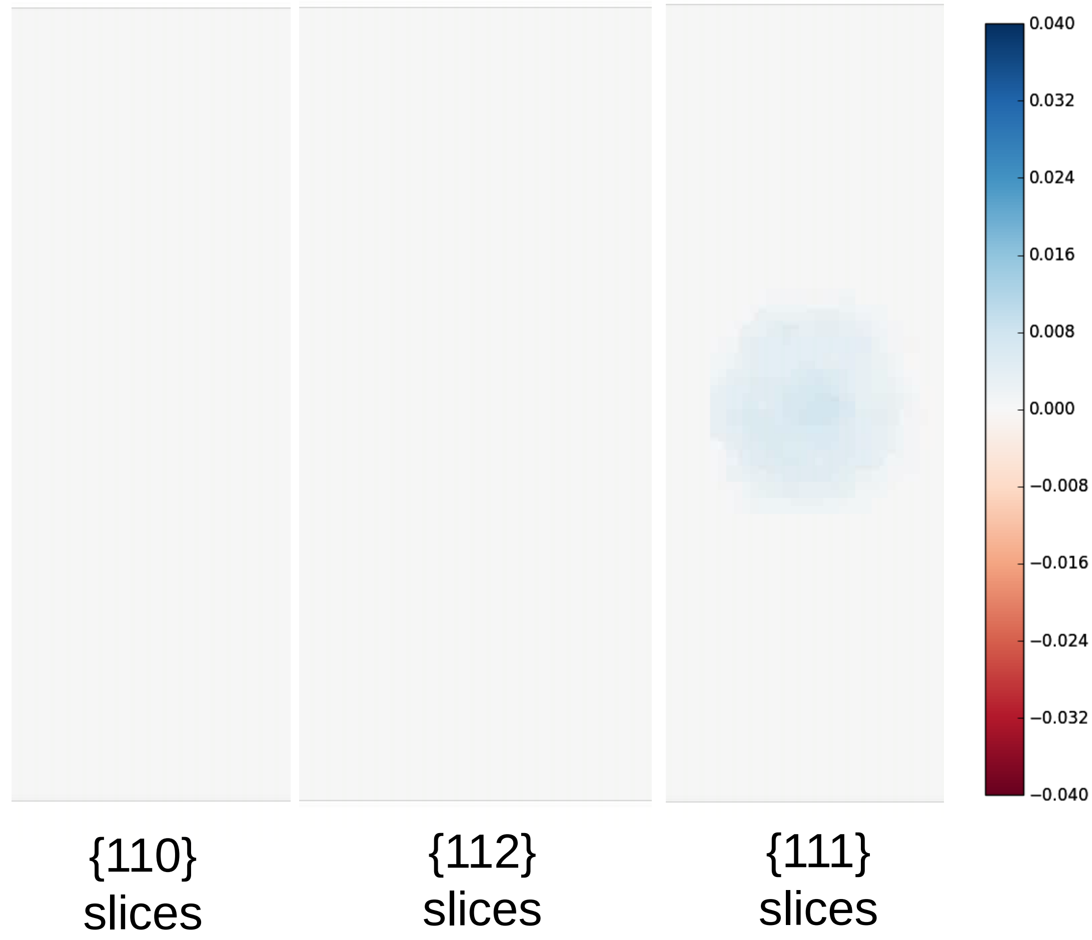

Summary

Materials are 3D – we should be doing something about that.

Crystallographic tomography is growing significantly in recent years with electron (and X-rays).

Questions?